CONFIDENTIAL

NACA RM A55A03

NACA

RESEARCH MEMORANDUM

EFFECTS OF SWEEP AND TAPER RATIO ON THE LONGITUDINAL CHARACTERISTICS OF AN ASPECT RATIO 3 WING-BODY COMBINATION AT MACH NUMBERS FROM 0.6 TO 1.4

By Earl D. Knechtel and James L. Summers

Ames Aeronautical Laboratory
Moffett Field, Calif.

CLASSIFIED DOCUMENT

NATIONAL ADVISORY COMMITTEE FOR AERONAUTICS

WASHINGTON

March 23, 1955

CONFIDENTIAL

NATIONAL ADVISORY COMMITTEE FOR AERONAUTICS

RESEARCH MEMORANDUM

EFFECTS OF SWEEP AND TAPER RATIO ON THE LONGITUDINAL CHARACTERISTICS OF AN ASPECT RATIO 3 WING-BODY COMBINATION AT MACH NUMBERS FROM 0.6 TO 1.4

By Earl D. Knechtel and James L. Summers

SUMMARY

An experimental investigation was conducted to assess the effects of sweep and taper ratio on the longitudinal characteristics of a wing-body combination at Mach numbers from 0.6 to 1.4 for a Reynolds number of 1.5×10^6. The wings were 3 percent thick and of aspect ratio 3. Leading-edge sweep was varied from 19.1° to 53.1° at a constant taper ratio of 0.4, and taper ratio was varied from 0 to 0.4 at a constant sweep angle of 53.1°.

Increased leading-edge sweep caused a progressive decrease not only of lift-curve slope, but also of the variation with Mach number of lift-curve slope and static longitudinal stability. Throughout the test Mach number range the minimum drag coefficient was less for 53.1° of sweep than for 19.1°. The drag-rise factor was generally larger and showed less variation with Mach number for the model having 53.1° of sweep. The maximum lift-drag ratio was higher for the model having 53.1° of sweep at supersonic Mach numbers.

Although the effects of taper ratio were less pronounced than those of sweep, the results of progressive increases in taper ratio, at a constant sweep angle of 53.1°, indicated that the model with 0.4 taper ratio had the least variation of lift-curve slope with Mach number for the three taper ratios investigated. Over-all change in static longitudinal stability was generally least for 0 taper ratio at 0 lift, and least for 0.4 taper ratio at 0.4 lift coefficient. The 0.4 taper ratio also resulted in a lower minimum drag coefficient and a higher maximum lift-drag ratio at Mach numbers above 0.95 than for the 0 taper ratio. In addition, the drag-rise factor is generally less and varies less with Mach number for the model having 0.4 taper ratio.

INTRODUCTION

The present investigation is part of a continuing program (refs. 1 and 2) directed toward assessing the effects of plan-form variations on the longitudinal characteristics of wing-body combinations at transonic Mach numbers. The study reported herein was conducted in the Ames 2- by 2-foot transonic wind tunnel to determine the longitudinal characteristics of five wing-body combinations having thin wings of aspect ratio 3 which embody systematic variations of sweep angle and taper ratio.

The results presented here have the twofold purpose of indicating the effects on the longitudinal characteristics of the models due to (1) variation of sweep at a constant moderate taper ratio, and (2) variation of taper ratio at a constant large angle of leading-edge sweep. Some of the results are compared with those of available theory.

NOTATION

C_D	drag coefficient
$C_{D_{min}}$	minimum drag coefficient
C_L	lift coefficient
C_{L_α}	lift-curve slope
C_m	pitching-moment coefficient referred to quarter-chord point of mean aerodynamic chord
c	local chord
$\bar{c}$	mean aerodynamic chord
$\frac{dC_m}{dC_L}$	slope of pitching-moment curve
$\Delta\left(\frac{dC_m}{dC_L}\right)$	change in pitching-moment-curve slope due to change in Mach number, $\Delta\left(\frac{dC_m}{dC_L}\right) = \frac{dC_m}{dC_L} - \left(\frac{dC_m}{dC_L}\right)_{M=0.6}$
$\left(\frac{L}{D}\right)_{max}$	maximum lift-drag ratio
l	body length, including portion removed to accommodate balance

M	free-stream Mach number
r	local radius of body
r_o	maximum radius of body
x	body longitudinal coordinate, measured from body nose
α	angle of attack, deg
Λ	sweepback angle of leading edge, deg
λ	taper ratio, $\frac{\text{tip chord}}{\text{root chord}}$

APPARATUS, TESTS, AND DATA REDUCTION

The investigation was conducted in the Ames 2- by 2-foot transonic wind tunnel, which is of the closed-circuit, variable-pressure type having maximum design operating conditions of 45 pounds per square inch absolute stagnation pressure and 120° F stagnation temperature. The wind tunnel is fitted with a flexible nozzle followed by a ventilated test section (fig. 1) which permits continuous choke-free operation from 0 to 1.4 Mach number.

Five wing-body models of steel were constructed such that sweep angle and taper ratio could be investigated independently for a constant aspect ratio of 3 (fig. 2). For three of the configurations the taper ratio was 0.4 and the leading-edge sweep angles, 19.1°, 45°, and 53.1°, while for the other two configurations the sweep angle was 53.1° and the taper ratios, 0 and 0.2. For the four wings having 45° and 53.1° of sweep, NACA 0003 airfoils were employed in the streamwise direction; whereas for the wing with 19.1° of sweep, biconvex sections 3 percent thick were utilized. The choice of profile for this latter case, for reasons discussed in reference 2, was based upon the known favorable drag characteristics of sharp leading edges for wings having leading edges supersonic over most of the supersonic Mach number range.

The models were mounted in the wind tunnel on a sting-supported internal strain-gage balance as shown in figures 1 and 3. The models spanned approximately 45 percent of the test section height and blocked approximately 0.5 percent of the cross-sectional area of the test section.

Lift and pitching moment were measured for all five models at angles of attack from -4° to approximately 13° at Mach numbers from 0.60 to 1.40. Drag was measured over the same ranges of angle of attack and Mach number for only three models. These were the configurations having 0.4 taper ratio with 19.1° and 53.1° of sweep, and the configuration having 0 taper

ratio with 53.1° of sweep. A Reynolds number of 1.5 million, based on the mean aerodynamic chord of each model, was held constant for the tests. All coefficients were based on the wing area including the portion within the body. The pitching-moment coefficient was based on the mean aerodynamic chord and referred to the quarter-chord point. The measured drag was adjusted to correspond to a condition of free-stream static pressure acting at the model base.

Subsonic wall interference corrections, calculated on the basis of the theory of reference 3, were found to be small and therefore were not applied to the data. No corrections were made for possible wall interference due to reflected waves at low supersonic speeds. These effects are discussed in the Results and Discussion section. Corrections for airstream angularity were not made, since they were found to be less than the probable errors in measuring angle of attack. Drag corrections due to longitudinal pressure gradient were unnecessary throughout the test Mach number range, since local Mach number deviations in the vicinity of the model were generally no greater than 0.003. The data have not been corrected for aeroelastic distortion.

Apart from the small systematic errors arising due to neglecting the corrections discussed above, certain random errors of measurement exist which determine the precision, or repeatability, of the data. An analysis was made of the precision of the Mach number, angle of attack, and coefficients of lift, pitching moment, and drag for the models of the present investigation, and the random uncertainties at three representative Mach numbers and two values of lift coefficient are presented in the following table:

	M = 0.8		M = 1.0		M = 1.2	
	$C_L = 0$	$C_L = 0.4$	$C_L = 0$	$C_L = 0.4$	$C_L = 0$	$C_L = 0.4$
M	±0.003	±0.003	±0.004	±0.004	±0.002	±0.002
α	±.02°	±.03°	±.02°	±.03°	±.02°	±.03°
C_L	±.005	±.010	±.005	±.006	±.003	±.006
C_m	±.004	±.006	±.004	±.005	±.003	±.005
C_D	±.0003	±.0010	±.0003	±.0006	±.0003	±.0006

RESULTS AND DISCUSSION

In figures 4 and 5 are shown, respectively, the variations of lift coefficient with angle of attack and with pitching-moment coefficient at Mach numbers from 0.60 to 1.40 for the five configurations tested. Drag results are presented in figure 6 for three of the configurations. The variations with Mach number of lift-curve slope and pitching-moment-curve slope for three values of lift coefficient are shown for the five configurations in figure 7. The small irregularities which appear in these curves at low supersonic speeds are believed to be the result of shock waves from the model which reflect from the tunnel walls and impinge upon the afterportion of the model. However, the influence of these reflected waves was confined to the Mach number range from 1.00 to 1.15 and was considered not large enough to affect the conclusions drawn from the data.

Variations of calculated lift-curve slope and pitching-moment-curve slope (whenever possible) with Mach number are shown in figure 7 for the zero-lift condition. These theoretical values include effects of wing-body interference as computed by the method of reference 4, which, in turn, is based upon theoretical wing-alone lift characteristics obtained from references 5, 6, and 7, respectively, for subsonic, sonic, and supersonic speeds. The experimental and calculated lift-curve slopes agreed within approximately 15 percent for all except the model having 53.1° sweep and 0.4 taper ratio. The poorer agreement in this case should not be surprising in view of the limitations of the interference theory with regard to swept trailing edges, and in view of the greater effects of aeroelastic distortion upon the more highly swept wing. In the two cases for which theoretical pitching-moment-curve slopes could be calculated, qualitative agreement between theory and experiment was noted for the model having the least sweep, whereas good agreement was obtained for the triangular-wing model. A consistent discrepancy between theory and experiment is noted in the Mach numbers at which peaks occur in the lift-curve slopes and pitching-moment-curve slopes. Peaks in the calculated curves occur at Mach numbers higher than those of the experimental curves by amounts varying from approximately 0.10 for the relatively unswept model down to approximately 0.03 for the triangular-wing model. This discrepancy probably results from the inability of the present linear theories to account for the fact that a local field of sonic and supersonic flow develops near the wing prior to the establishment of these conditions in the free stream.

Effect of Sweep

Lift and pitching-moment characteristics.- In figure 8 a comparison of the lift-curve slopes obtained for the three sweep angles reveals no unusual trends. With increased sweep, the lift-curve slope not only became smaller, but also varied less rapidly with Mach number.

In figure 8 for the three sweep angles investigated a comparison is shown of the change in static longitudinal stability from that obtained at the same lift coefficient at 0.6 Mach number. Comparison on this basis makes evident the large effects of sweep on the variation of longitudinal stability with Mach number. At high subsonic Mach numbers the model having 19.1° of sweep underwent rapid changes in static longitudinal stability; whereas the models having greater sweep generally exhibited a smoother variation of stability with Mach number. The generally superior stability characteristics at lift coefficients up to 0.4 for 53.1° of sweep may be somewhat offset, however, by the pitch-up tendencies at larger lift coefficients in the high subsonic speed range. (See fig. 5(c).)

Drag characteristics.- In figure 9 the variations with Mach number of minimum drag coefficient, drag-rise factor, and maximum lift-drag ratio are compared for sweep angles of 19.1° and 53.1°. Throughout the test Mach number range the minimum drag coefficient was less for the wing having the larger sweep angle, the amount of this difference being as great as 40 percent at sonic speed.

Drag-rise factor was determined by the slope of curves of drag coefficient plotted against lift coefficient squared, over the linear range of these curves from 0 to 0.4 lift coefficient. The drag-rise factor was generally larger and varied less with Mach number for the model having the greater sweep angle.

Maximum lift-drag ratios were attained at lift coefficients from 0.20 to 0.25. The variation of maximum lift-drag ratio with Mach number shown in figure 9 generally reflects the corresponding variations of minimum drag coefficient and drag-rise factor. Increase in sweep angle from 19.1° to 53.1° resulted in slight decreases in maximum lift-drag ratio at Mach numbers from 0.75 to 0.95 and increases of as much as 15 percent at supersonic Mach numbers.

Effect of Taper Ratio

Lift and pitching-moment characteristics.- A comparison is shown in figure 10 of the slopes of the lift and moment curves for the three taper ratios. Although the effect of taper was not large, the variation with Mach number of lift-curve slope was generally least for the configuration having 0.4 taper ratio. In general, the over-all change in static longitudinal stability was least for 0 taper ratio at 0 lift coefficient and least for 0.4 taper ratio at 0.4 lift coefficient.

Drag characteristics.- The variations with Mach number of minimum drag coefficient, drag-rise factor, and maximum lift-drag ratio are shown in figure 11 for the swept wings having taper ratios of 0 and 0.4. These results indicate that up to 0.95 Mach number the minimum drag coefficients

and maximum lift-drag ratios for the two models compare quite closely. At Mach numbers above 0.95, however, lower minimum drag coefficients and higher maximum lift-drag ratios are realized for the 0.4 taper ratio. The drag-rise factor for the model having 0.4 taper ratio is generally less and varies less with Mach number than for the model with 0 taper ratio.

Comparison with Results of Reference 1

The models for which longitudinal characteristics were presented in reference 1 had an unswept midchord line, NACA 64A003 streamwise sections, and taper ratios varying from 1.0 to 0. Accordingly, the leading-edge sweep angle varied from 0° to 33.7°, and it may be of interest to compare the effect of the sweep variations of reference 1 with the corresponding effect indicated in the present report. Such data comparisons are made in figures 9 and 12 for two configurations of reference 1 and the most nearly comparable models of the present investigation for which corresponding data were obtained.

In figure 12 the variations with Mach number of lift-curve slope and pitching-moment-curve slope are shown for two models of the present investigation having 19.1° and 45.0° of sweep and two models of reference 1 having 12.6° and 33.7° of sweep. The effect of leading-edge sweep was quite similar in the two cases, the variations with Mach number of both lift-curve slope and pitching-moment-curve slope generally becoming less abrupt with increasing sweep angle.

In figure 9 the variations with Mach number of minimum drag coefficient, drag-rise factor, and maximum lift-drag ratio for the same two models of reference 1 are compared with the corresponding results for the models of the present investigation having a taper ratio of 0.4 and leading-edge sweep angles of 19.1° and 53.1°. The difference in maximum lift-drag ratios at subsonic Mach numbers between the two models having the least sweep is attributable to the use of a sharp leading-edge, and a consequent loss of leading-edge suction, for the model having 19.1° of sweep. Generally, however, the effect of leading-edge sweep on the drag characteristics, as on the slopes of the lift and pitching-moment curves, was much the same for the models of reference 1 as for the models of the present investigation. These comparisons suggest the possibility that the effects in reference 1 attributed to taper ratio might have been due in part to leading-edge sweep.

CONCLUSIONS

An experimental investigation was conducted to determine the effects of sweep and taper ratio on the lift, pitching-moment, and drag characteristics of an aspect ratio 3 wing-body combination at Mach numbers from 0.6 to 1.4, at 1.5×10^6 Reynolds number. Results obtained for wings having leading-edge sweep angles of 19.1°, 45°, and 53.1° at 0.4 taper ratio and for wings having taper ratios of 0, 0.2, and 0.4 at 53.1° of sweep lead to the following conclusions:

1. Increased sweep resulted in progressive decreases in lift-curve slope as well as in reduced variation with Mach number of the lift-curve slope and static longitudinal stability.

2. An increase of sweep from 19.1° to 53.1° led to generally decreased minimum drag coefficient and increased drag-rise factor, and to increased maximum lift-drag ratio at Mach numbers above 0.94.

3. Increased taper ratio resulted in a slightly reduced variation of lift-curve slope with Mach number, a somewhat larger over-all change in static longitudinal stability with Mach number at 0 lift, and a slightly smaller change in stability with Mach number at 0.4 lift coefficient.

4. An increase of taper ratio from 0 to 0.4 resulted in lower minimum drag coefficient and higher maximum lift-drag ratio at Mach numbers above 0.95, and generally a reduction both in magnitude and in variation of drag-rise factor with Mach number.

Ames Aeronautical Laboratory
National Advisory Committee for Aeronautics
Moffett Field, Calif., Jan. 3, 1955

REFERENCES

1. Summers, James L., Treon, Stuart L., and Graham, Lawrence A.: Effects of Taper Ratio on the Longitudinal Characteristics at Mach Numbers from 0.6 to 1.4 of a Wing-Body-Tail Combination Having an Unswept Wing of Aspect Ratio 3. NACA RM A54L20, 1954.

2. Hall, Charles F.: Lift, Drag, and Pitching Moment of Low-Aspect-Ratio Wings at Subsonic and Supersonic Speeds. NACA RM A53A30, 1953.

3. Baldwin, Barrett S., Turner, John B., and Knechtel, Earl D.: Wall Interference in Wind Tunnels with Slotted and Porous Boundaries at Subsonic Speeds. NACA TN 3176, 1954.

4. Nielsen, Jack N., Kaattari, George E., and Anastasio, Robert F.: A Method for Calculating the Lift and Center of Pressure of Wing-Body-Tail Combinations at Subsonic, Transonic, and Supersonic Speeds. NACA RM A53G08, 1953.

5. DeYoung, John, and Harper, Charles W.: Theoretical Symmetric Span Loading at Subsonic Speeds for Wings Having Arbitrary Plan Form. NACA Rep. 921, 1948.

6. Jones, Robert T.: Properties of Low-Aspect-Ratio Pointed Wings at Speeds Below and Above the Speed of Sound. NACA Rep. 835, 1946.

7. Lapin, Ellis: Charts for the Computation of Lift and Drag of Finite Wings at Supersonic Speeds. Douglas Aircraft Co. Rep. SM-13480, Oct. 1949.

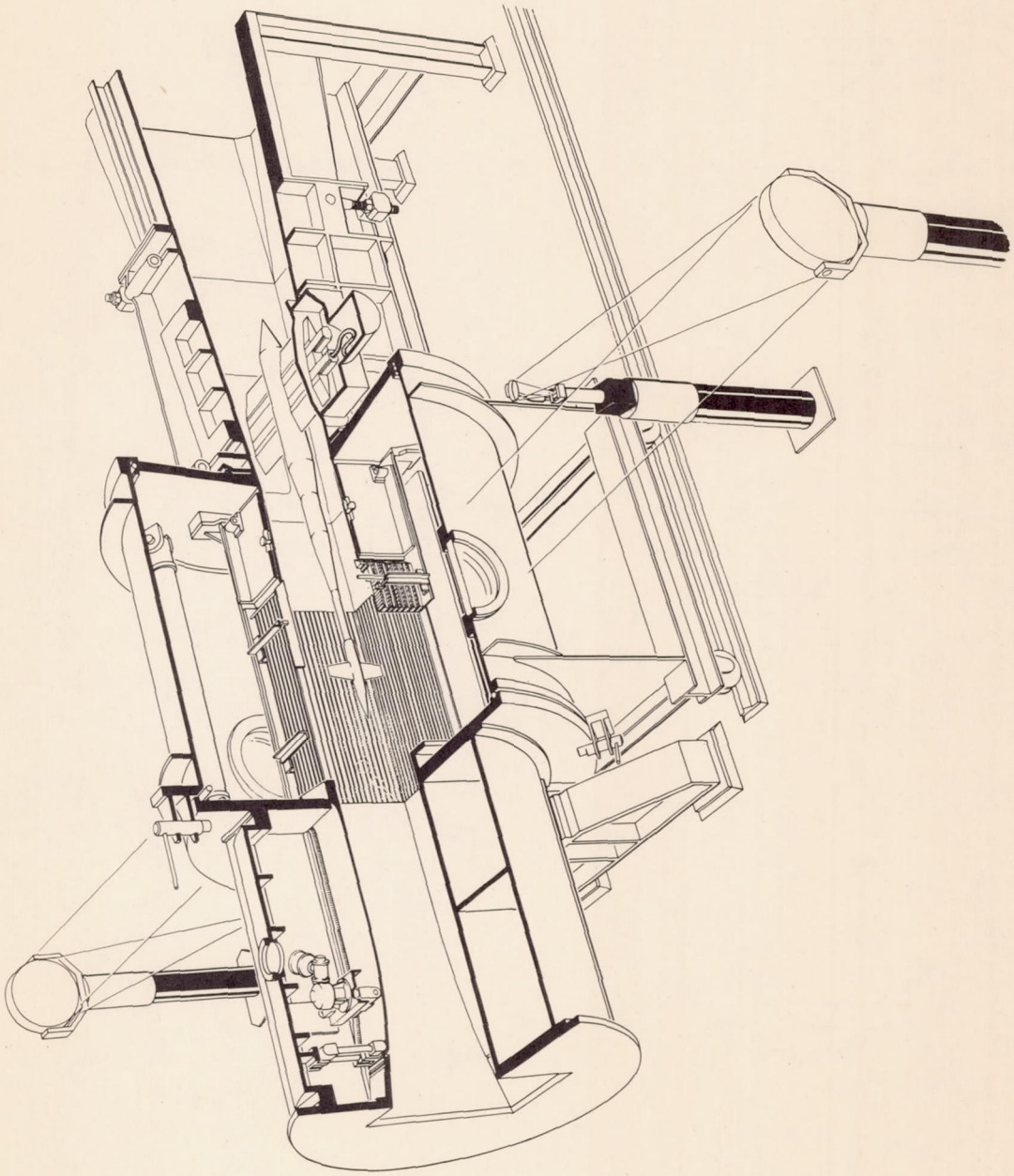

Figure 1.- The Ames 2-by 2-foot transonic wind tunnel.

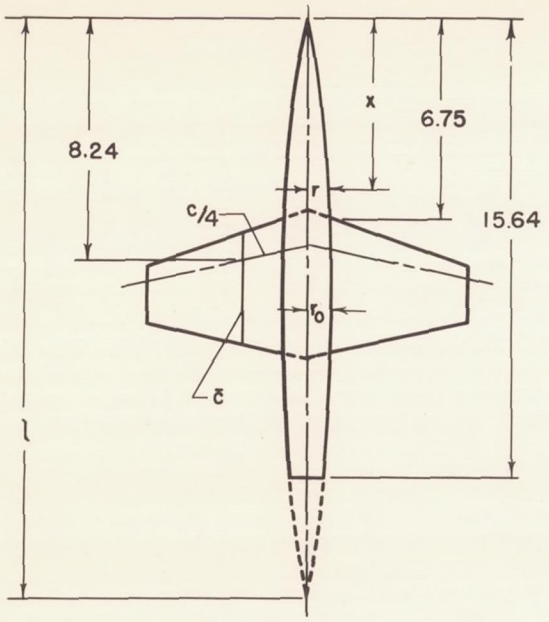

$\Lambda = 19.1°$

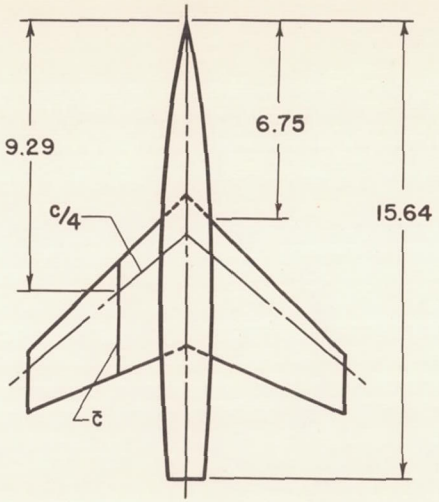

$\Lambda = 45.0°$

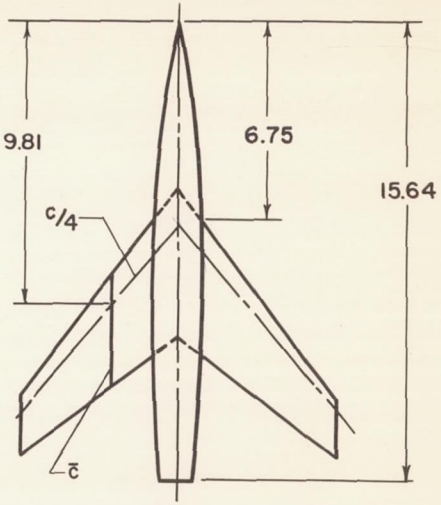

$\Lambda = 53.1°$

Equation of body radii:

$$\frac{r}{r_0} = \left[1-\left(1-\frac{2x}{l}\right)^2\right]^{3/4}$$

$l = 19.83$

$r_0 = 0.79$

(Dimensions in inches except as noted)

Leading-edge sweep	19.1°	45.0°	53.1°
Taper ratio	0.39	0.40	0.40
Aspect ratio	3.09	3.0	3.0
Airfoil section (streamwise)	3% biconvex	NACA 0003	NACA 0003
Area	38.87 sq in.	38.88 sq in.	38.88 sq in.
Span	10.95	10.80	10.80
Mean aerodynamic chord	3.78	3.82	3.82
Tip chord	1.99	2.06	2.06
Root chord (at centerline)	5.11	5.14	5.14

(a) Sweep-angle variations.

Figure 2.- Dimensions of the wing-body configurations.

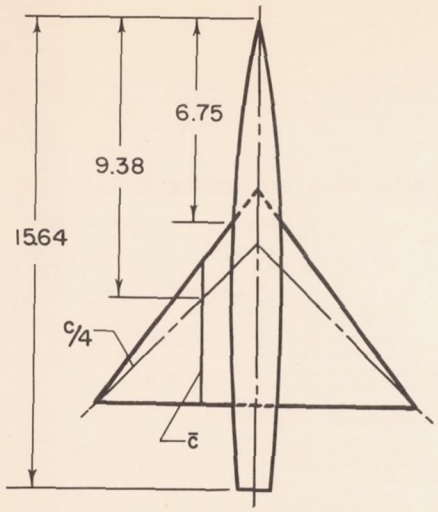

λ = 0

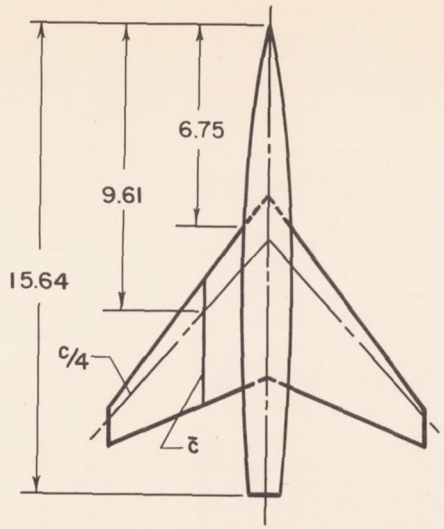

λ = 0.2

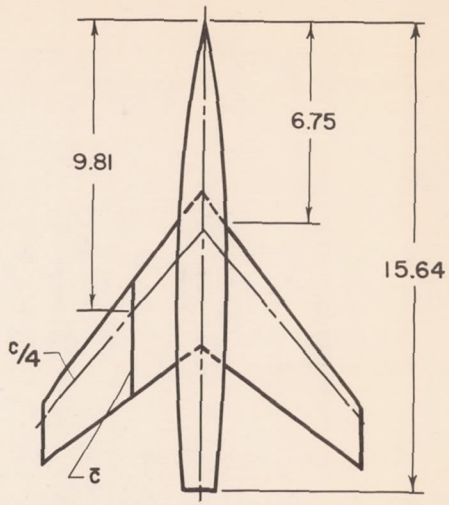

λ = 0.4

Taper ratio	0	0.2	0.4
Leading-edge sweep	53.1°	53.1°	53.1°
Aspect ratio	3.0	3.0	3.0
Airfoil section (streamwise)	NACA 0003	NACA 0003	NACA 0003
Area	38.88 sq in.	38.88 sq in.	38.88 sq in.
Span	10.80	10.80	10.80
Mean aerodynamic chord	4.80	4.13	3.82
Tip chord	0	1.20	2.06
Root chord (at centerline)	7.20	6.00	5.14

(Dimensions in inches except as noted)

(b) Taper-ratio variations.

Figure 2.- Concluded.

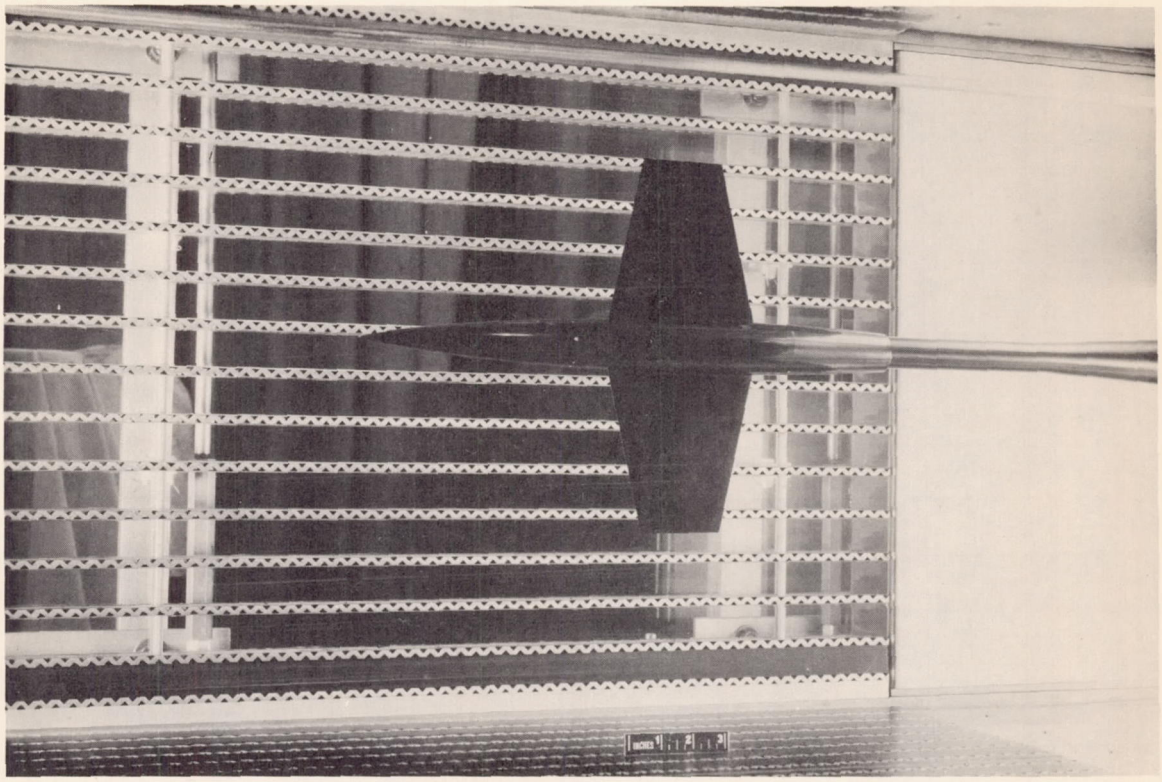

A-19209

Figure 3.- Typical model installation in the Ames 2- by 2-foot transonic wind tunnel.

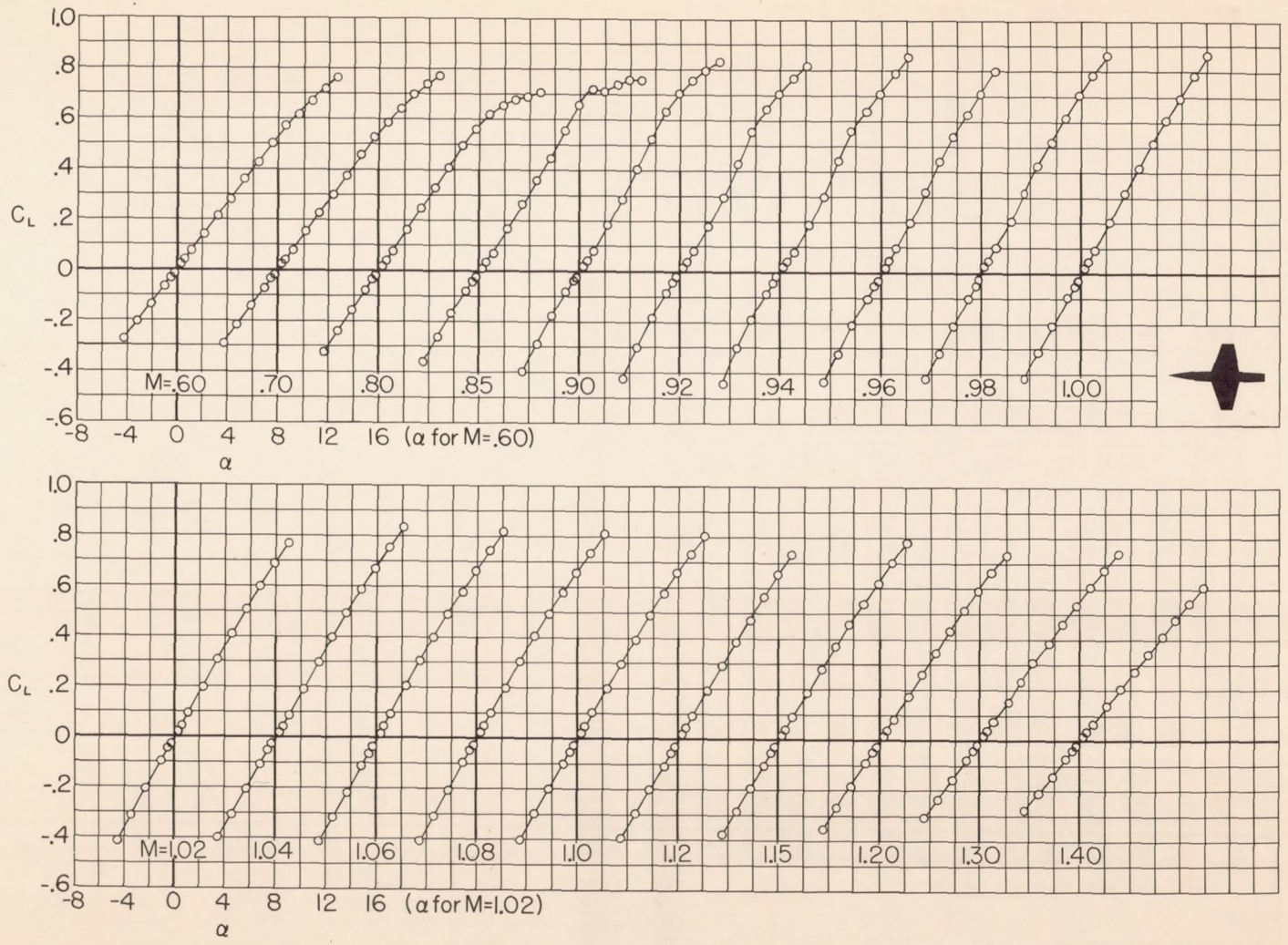

(a) $\Lambda = 19.1°$, $\lambda = 0.4$.

Figure 4.-Variation of lift coefficient with angle of attack at constant Mach number.

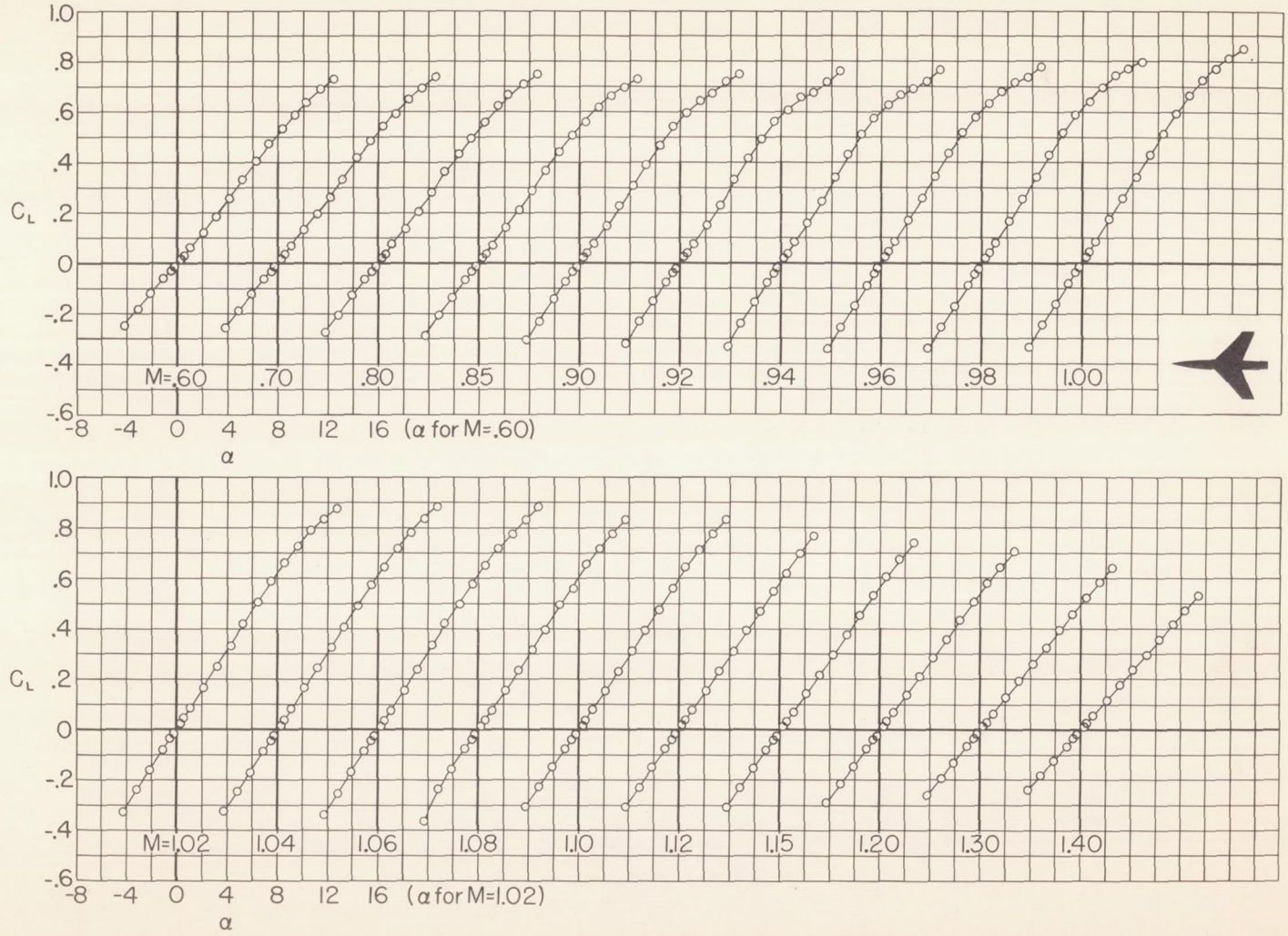

(b) $\Lambda = 45.0°$, $\lambda = 0.4$.

Figure 4.- Continued.

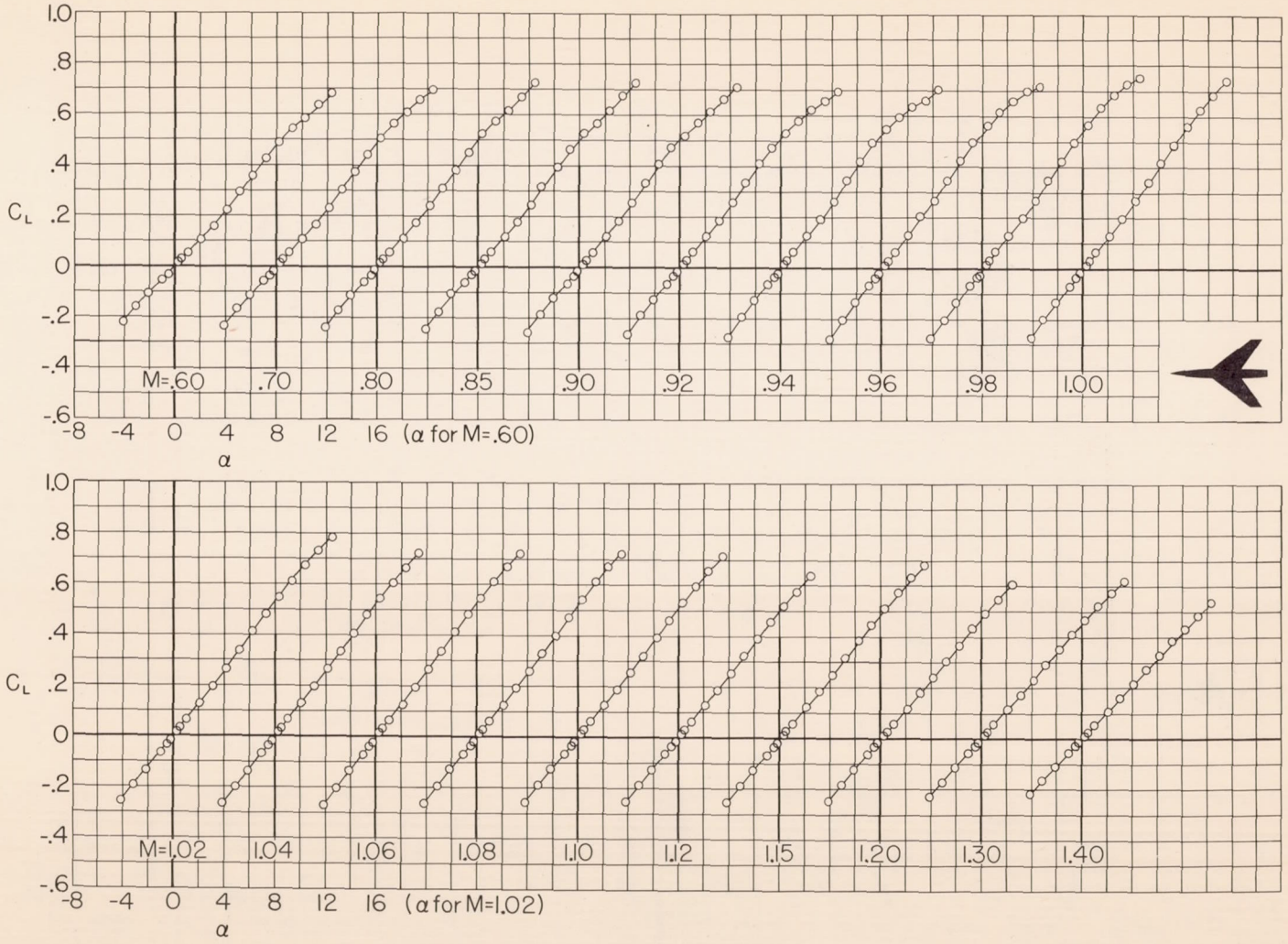

(c) $\Lambda = 53.1°$, $\lambda = 0.4$.

Figure 4.- Continued.

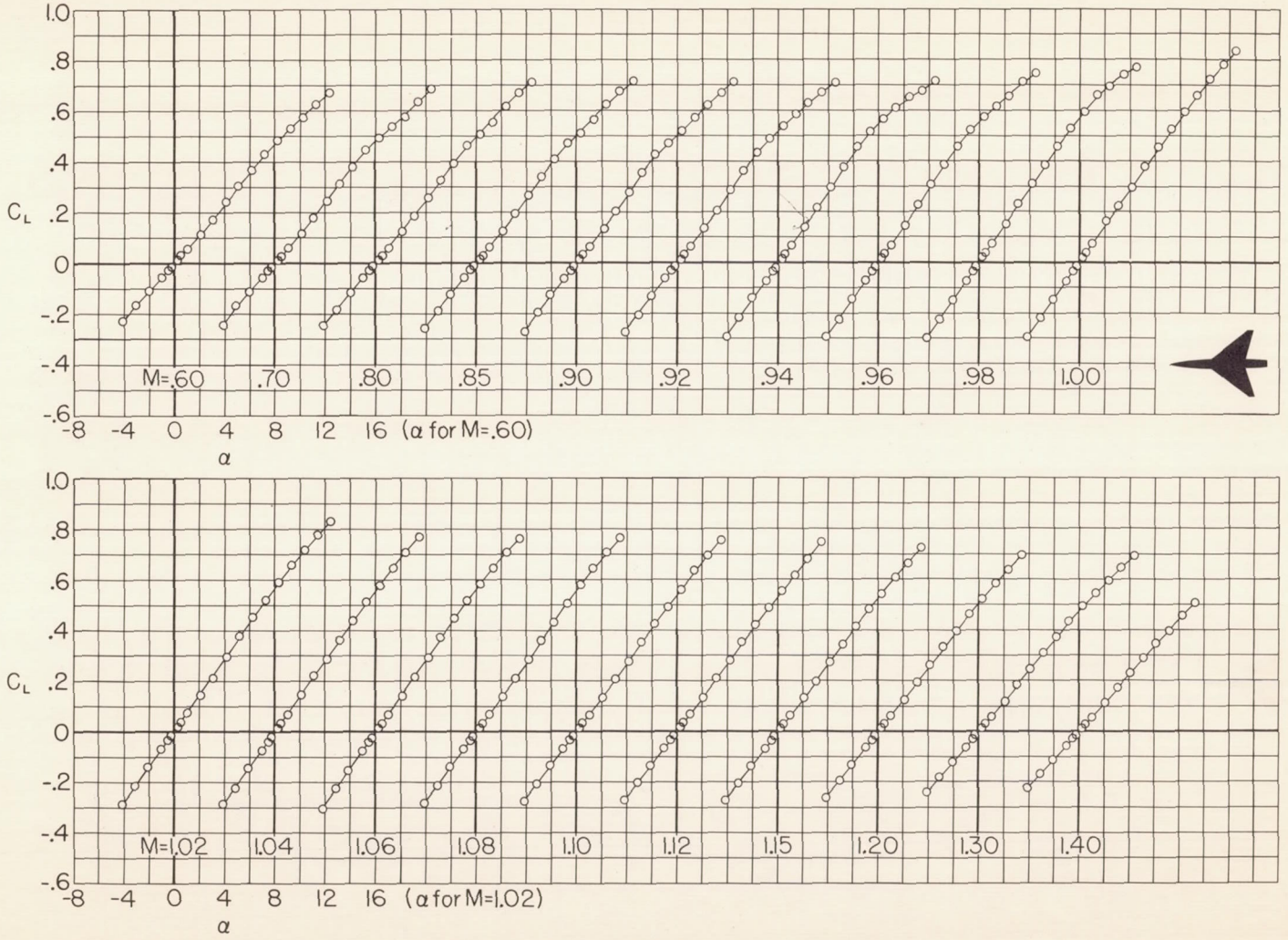

(d) $\Lambda = 53.1°$, $\lambda = 0.2$.

Figure 4.- Continued.

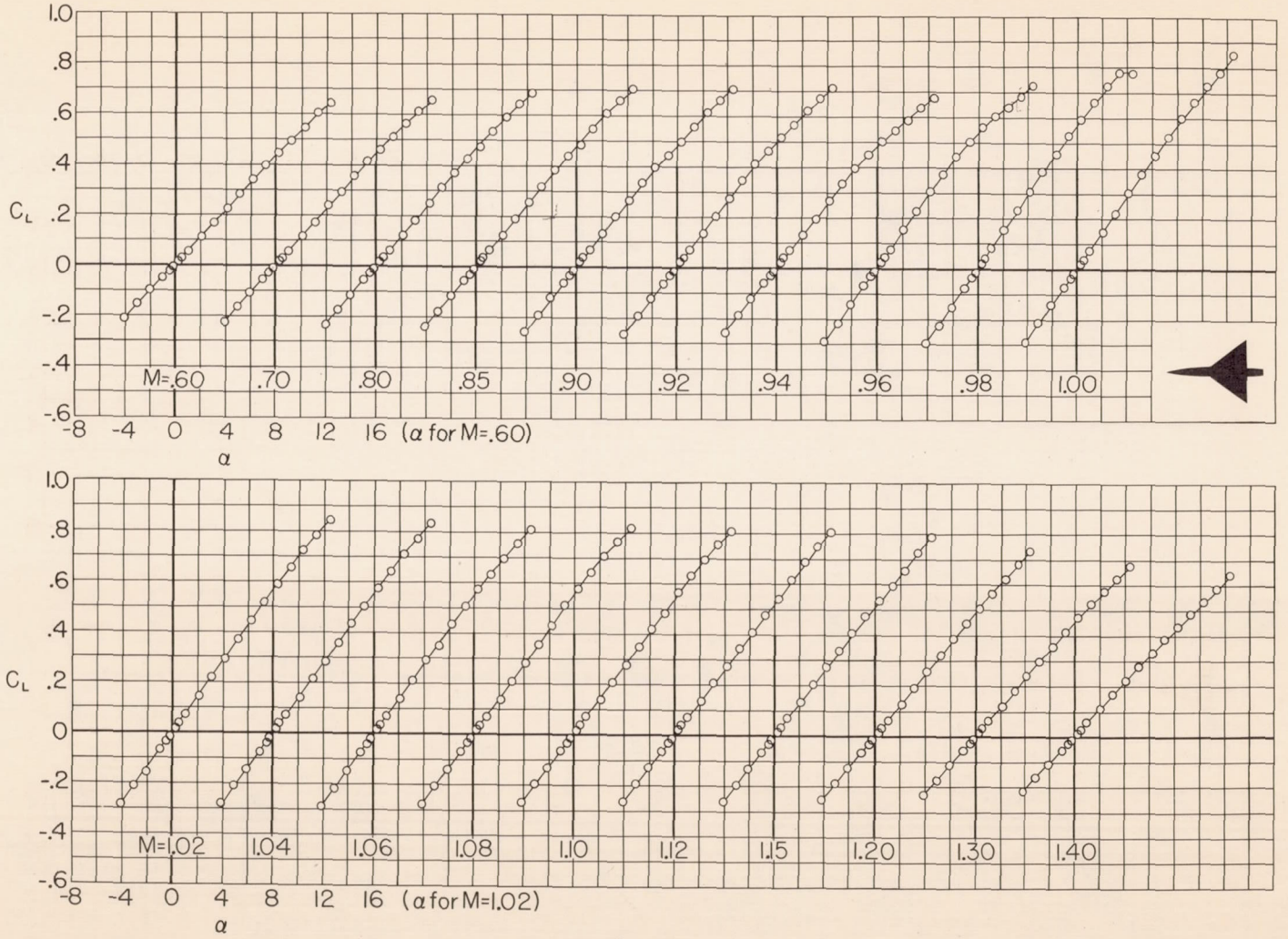

(e) $\Lambda = 53.1°$, $\lambda = 0$.

Figure 4.- Concluded.

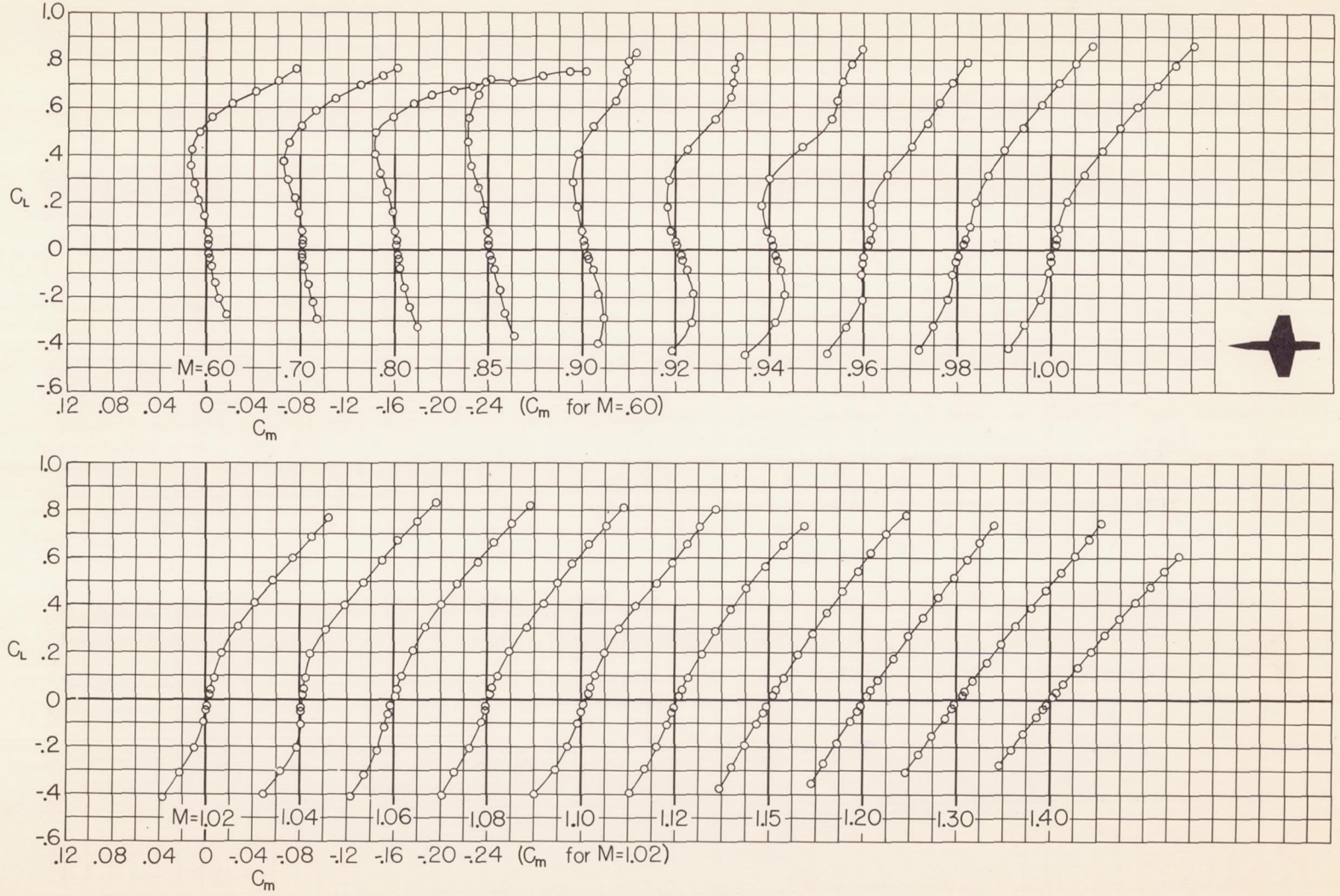

(a) $\Lambda = 19.1°$, $\lambda = 0.4$.

Figure 5.- Variation of pitching-moment coefficient with lift coefficient at constant Mach number.

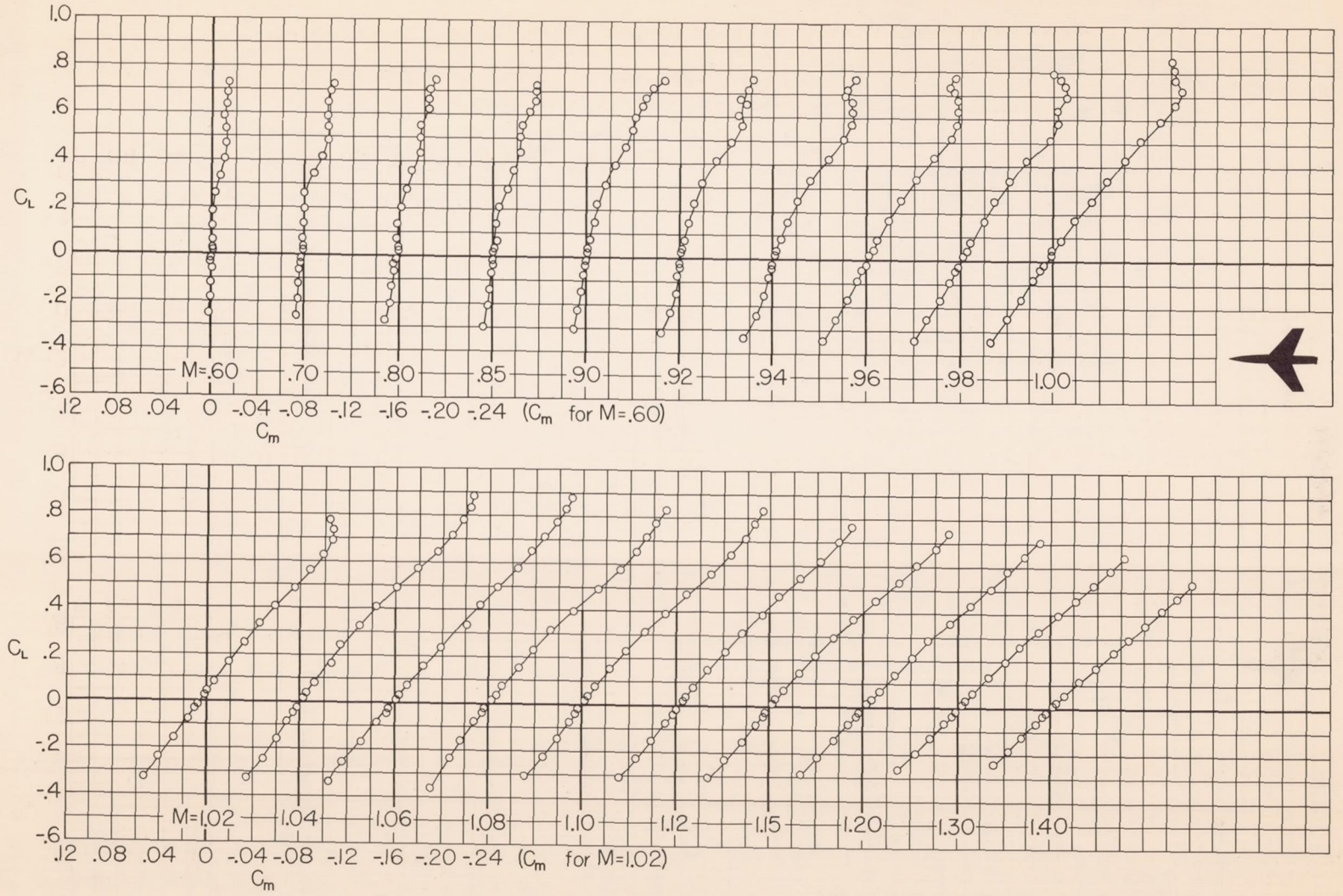

(b) $\Lambda = 45°$, $\lambda = 0.4$.

Figure 5.- Continued.

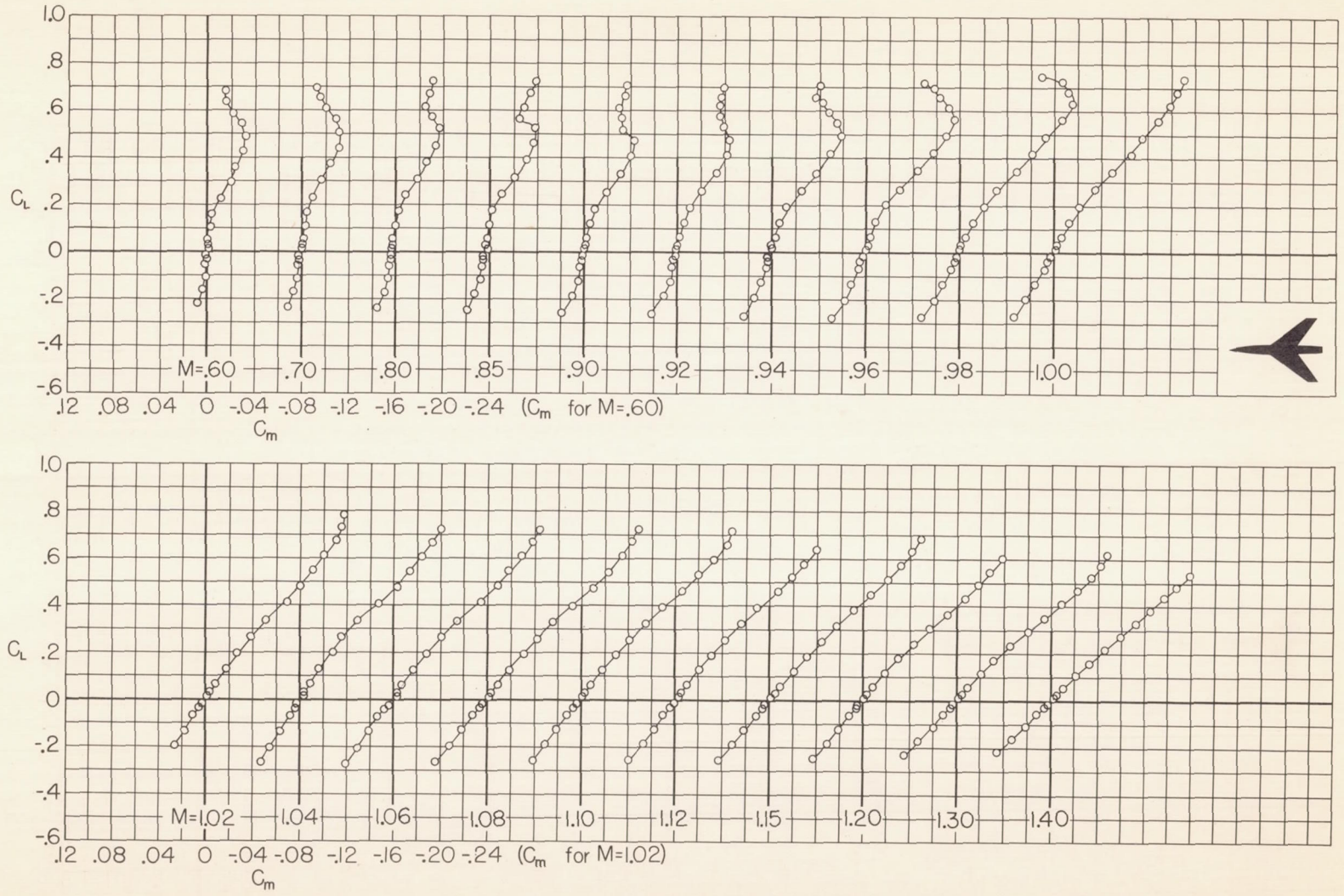

(c) $\Lambda = 53.1°$, $\lambda = 0.4$.

Figure 5.- Continued.

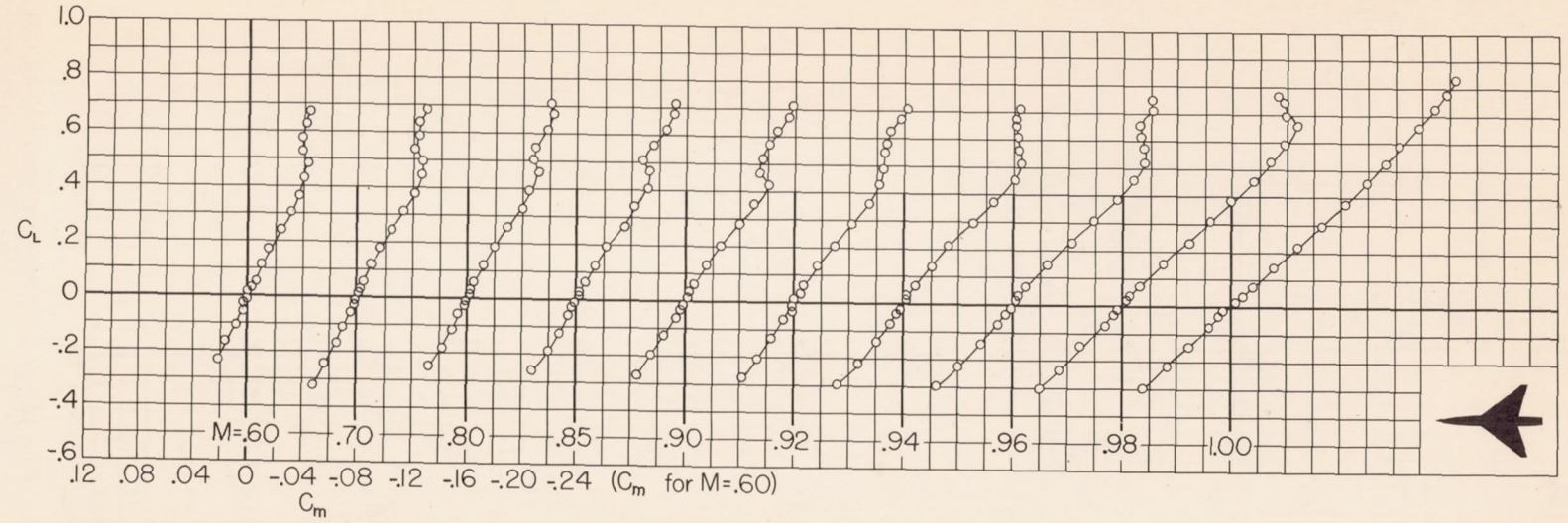

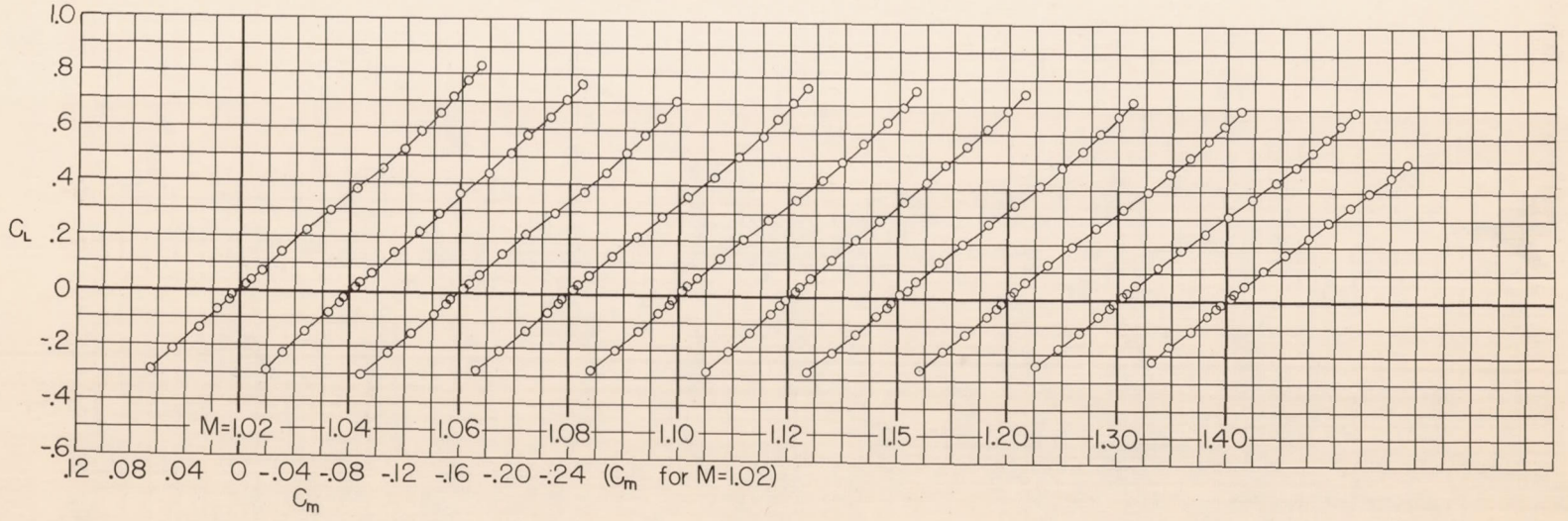

(d) $\Lambda = 53.1°$, $\lambda = 0.2$.

Figure 5.- Continued.

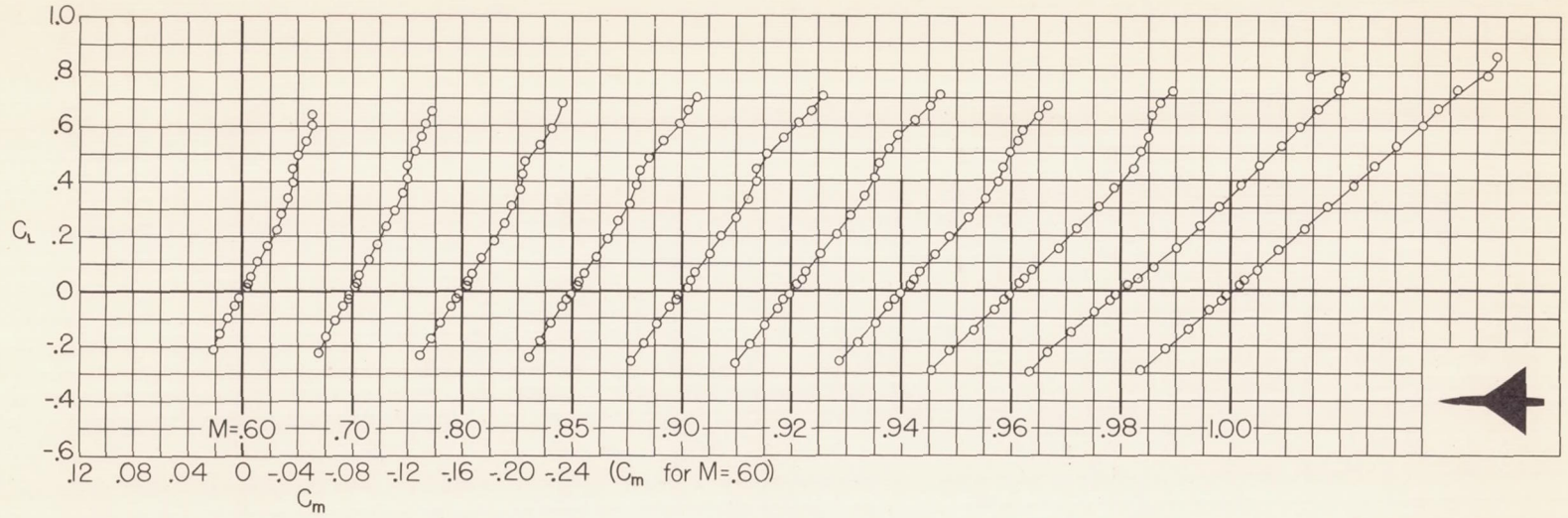

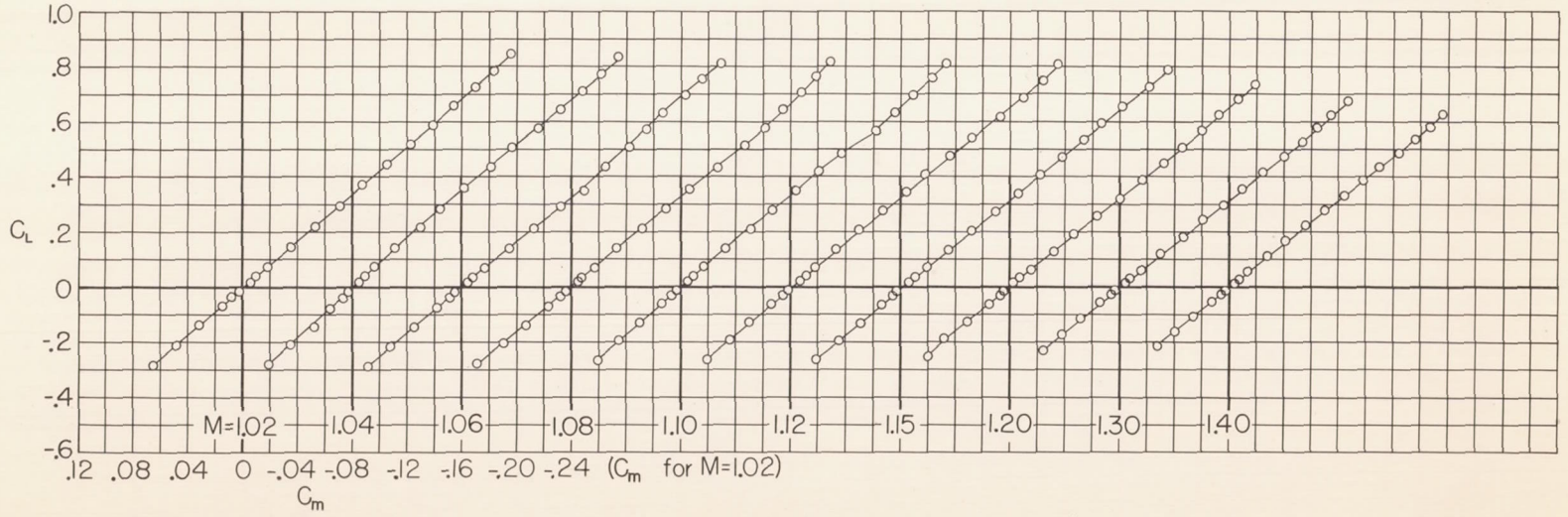

(e) $\Lambda = 53.1°$, $\lambda = 0$.

Figure 5.- Concluded.

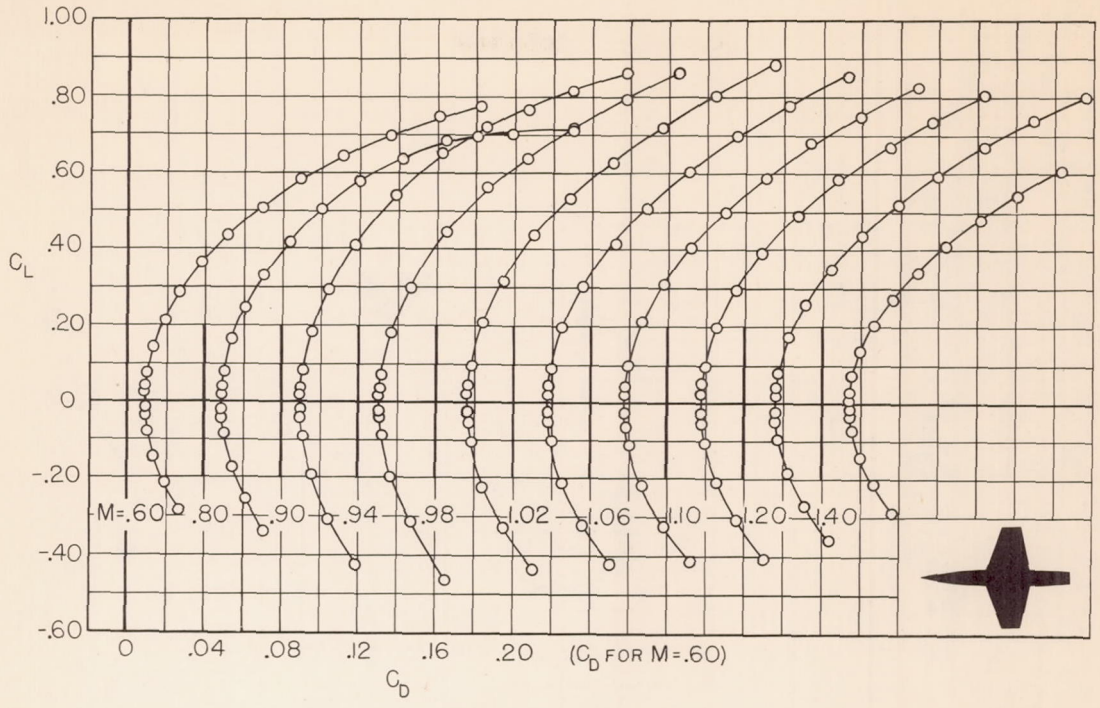

(a) $\Lambda = 19.1°$, $\lambda = 0.4$.

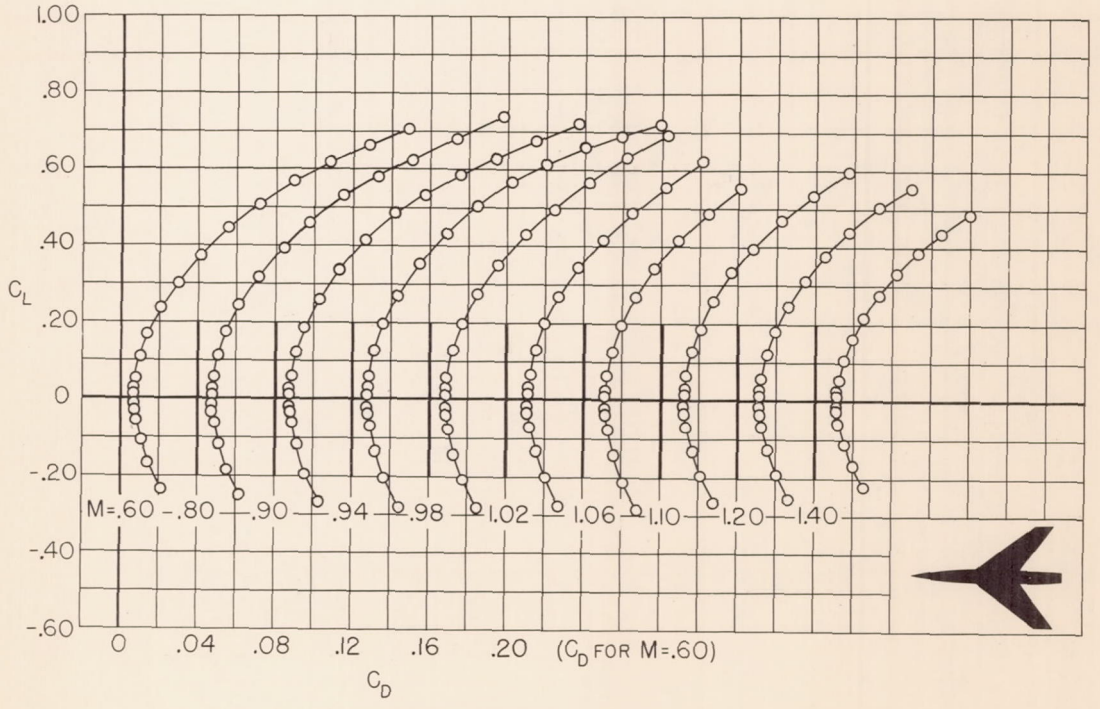

(b) $\Lambda = 53.1°$, $\lambda = 0.4$.

Figure 6.- Variation of drag coefficient with lift coefficient at constant Mach number.

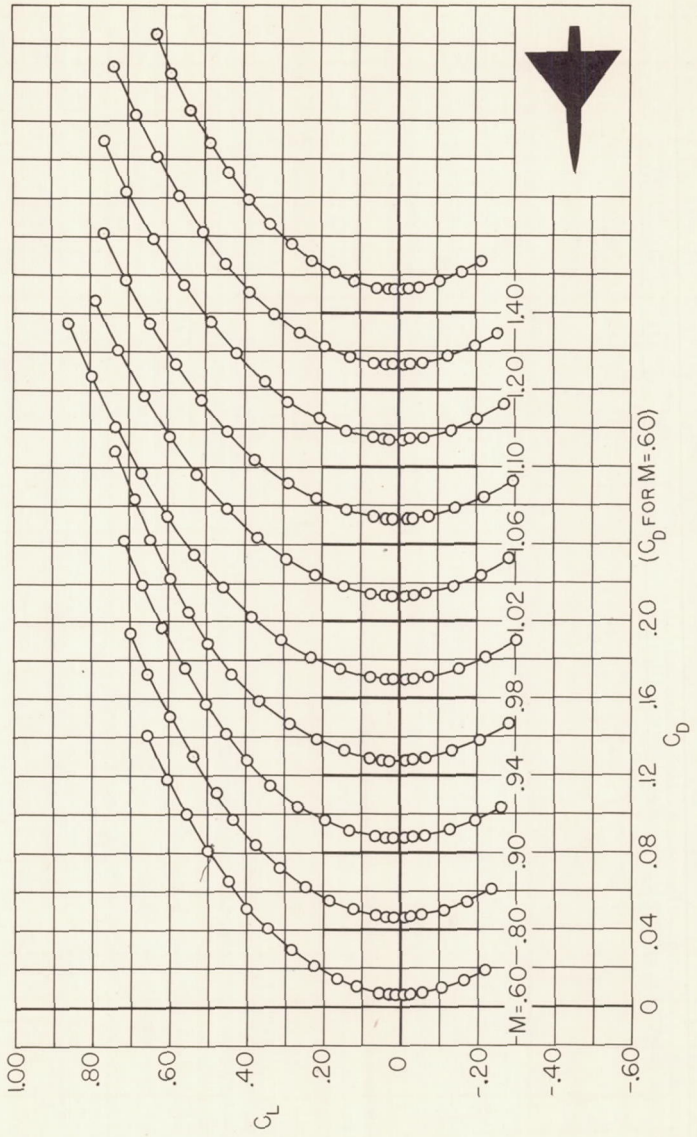

(c) $\Lambda = 53.1°$, $\lambda = 0$.

Figure 6.- Concluded.

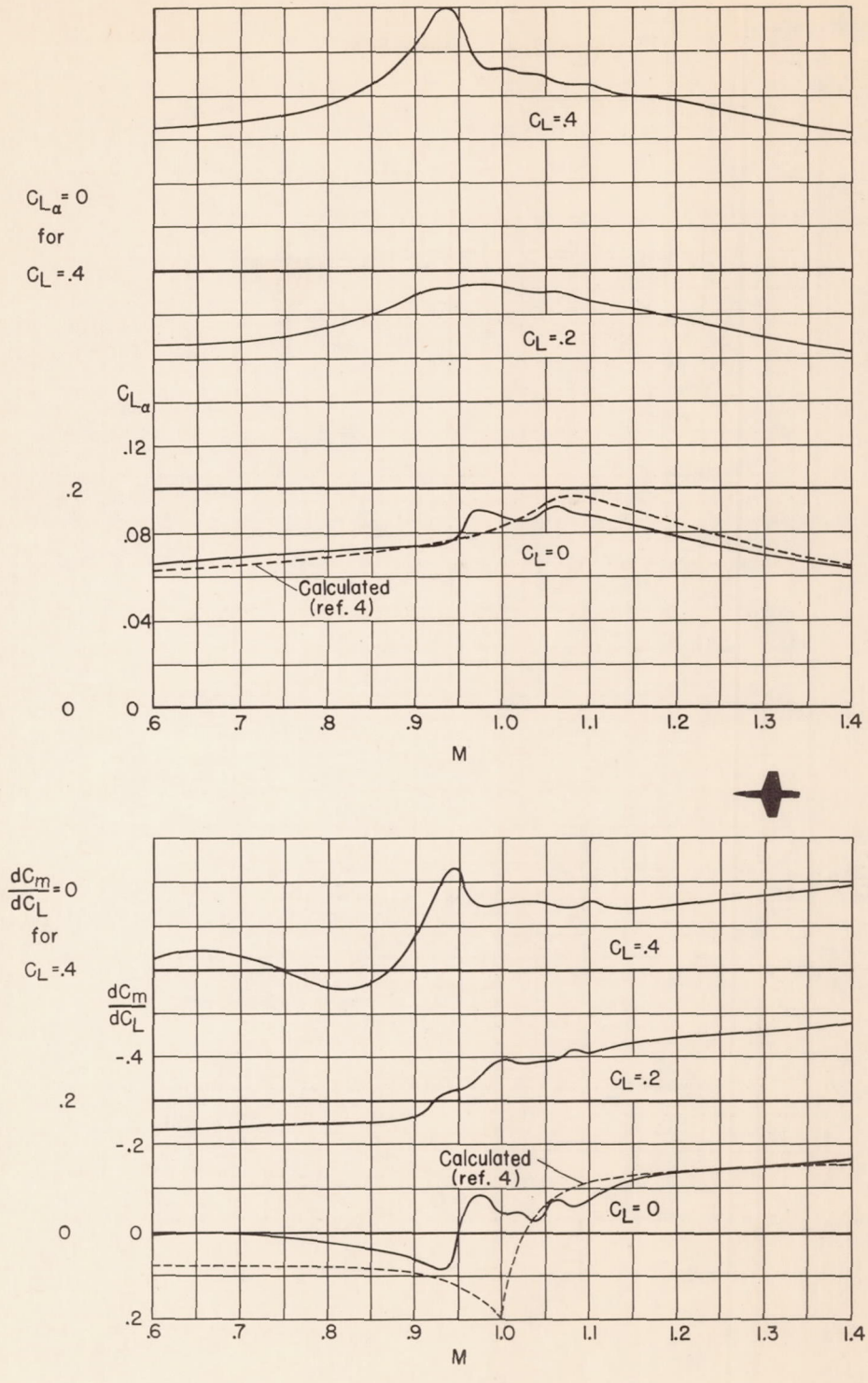

(a) $\Lambda = 19.1°$, $\lambda = 0.4$.

Figure 7.- Variation of lift-curve slope and pitching-moment-curve slope with Mach number.

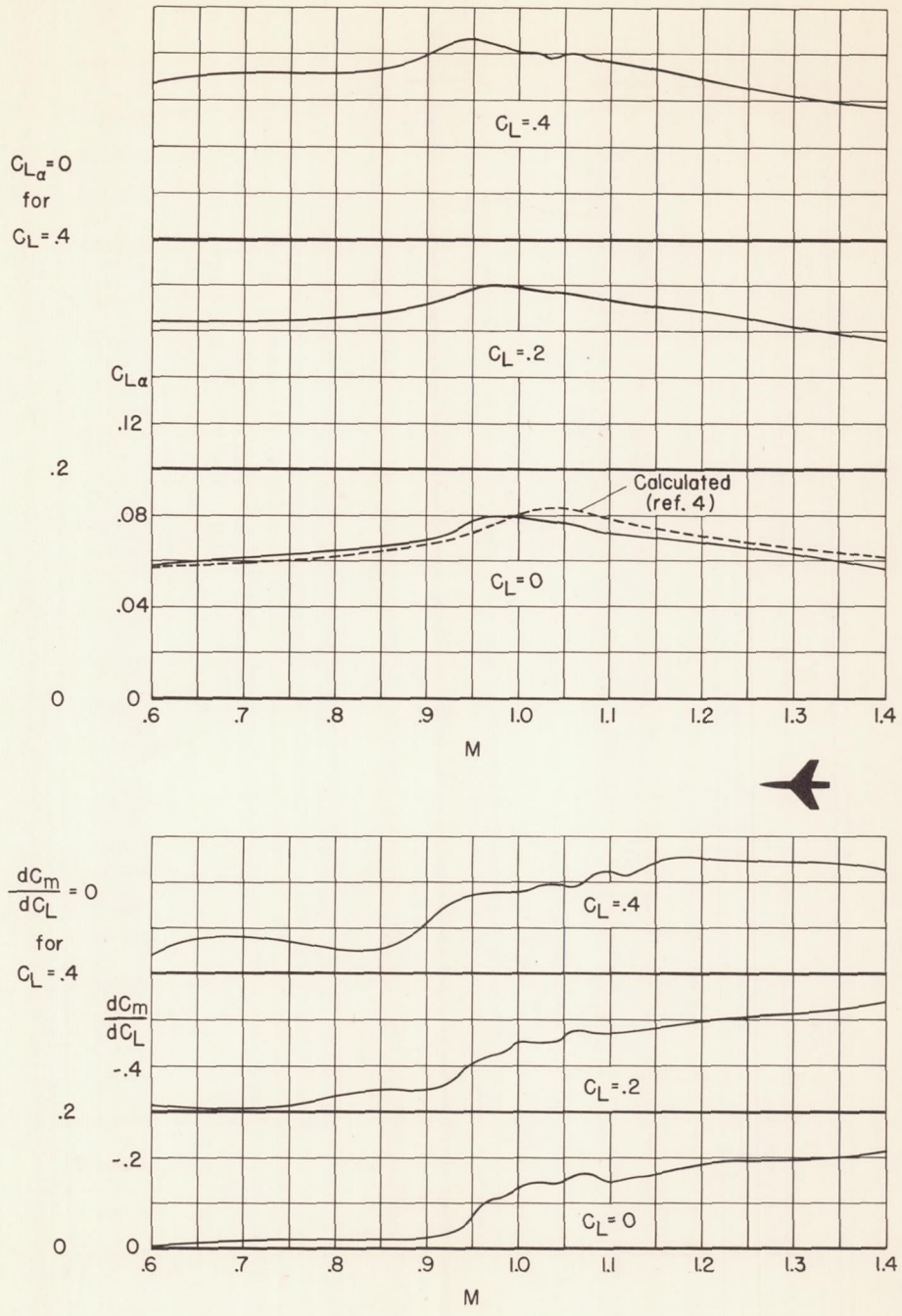

(b) $\Lambda = 45.0$, $\lambda = 0.4$.

Figure 7.- Continued.

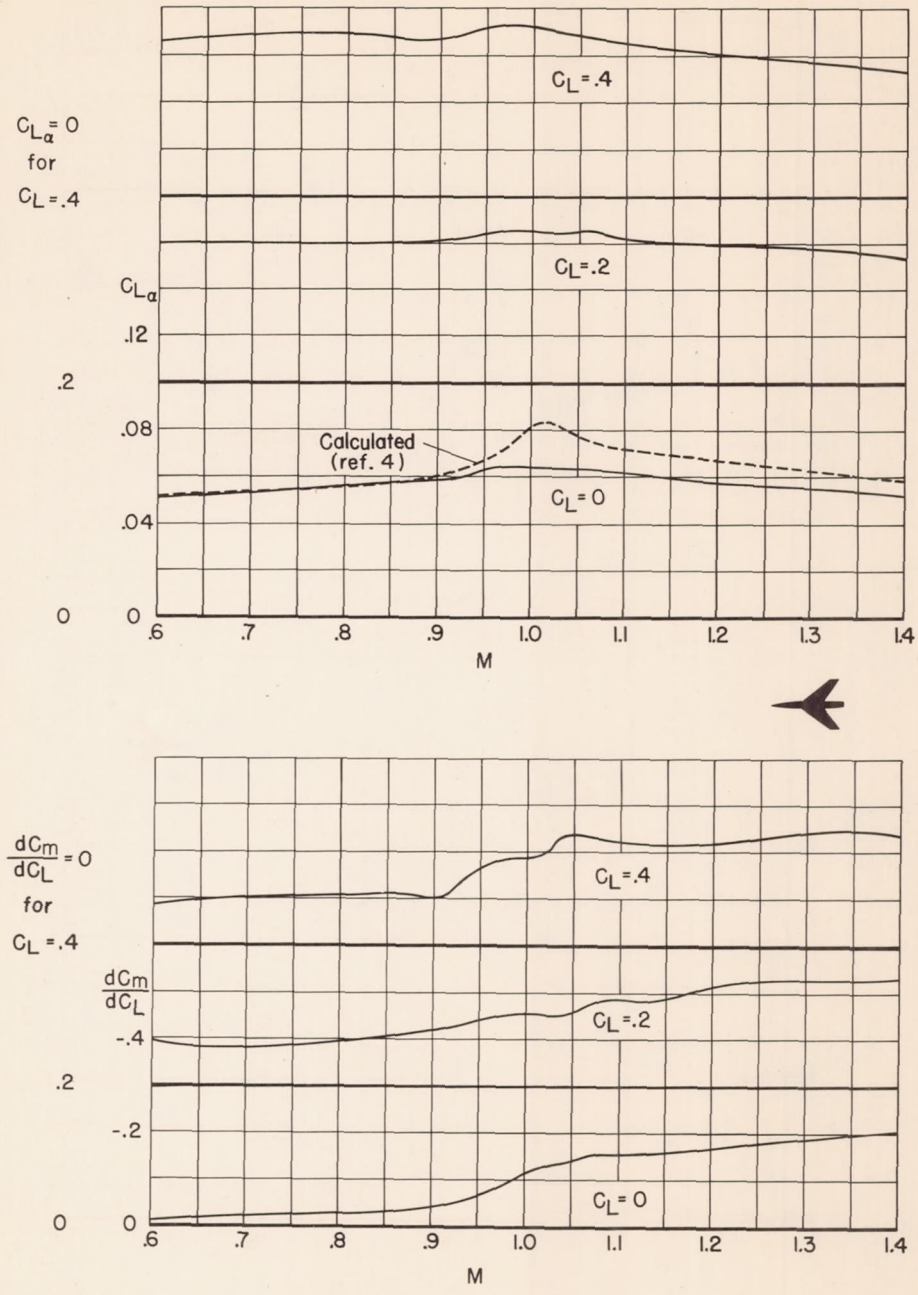

(c) $\Lambda = 53.1$, $\lambda = 0.4$.

Figure 7.- Continued.

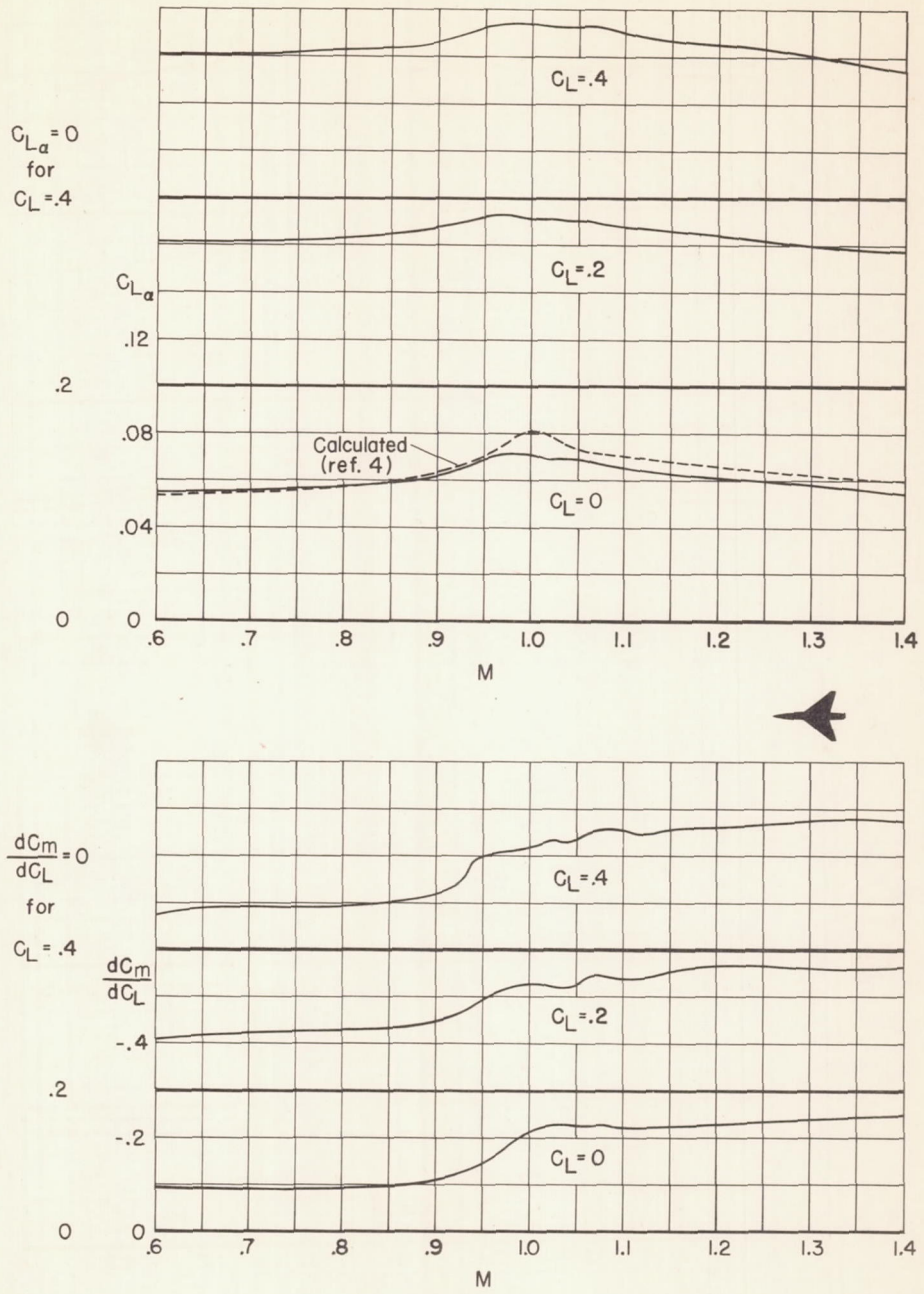

(d) $\Lambda = 53.1$, $\lambda = 0.2$.

Figure 7.- Continued.

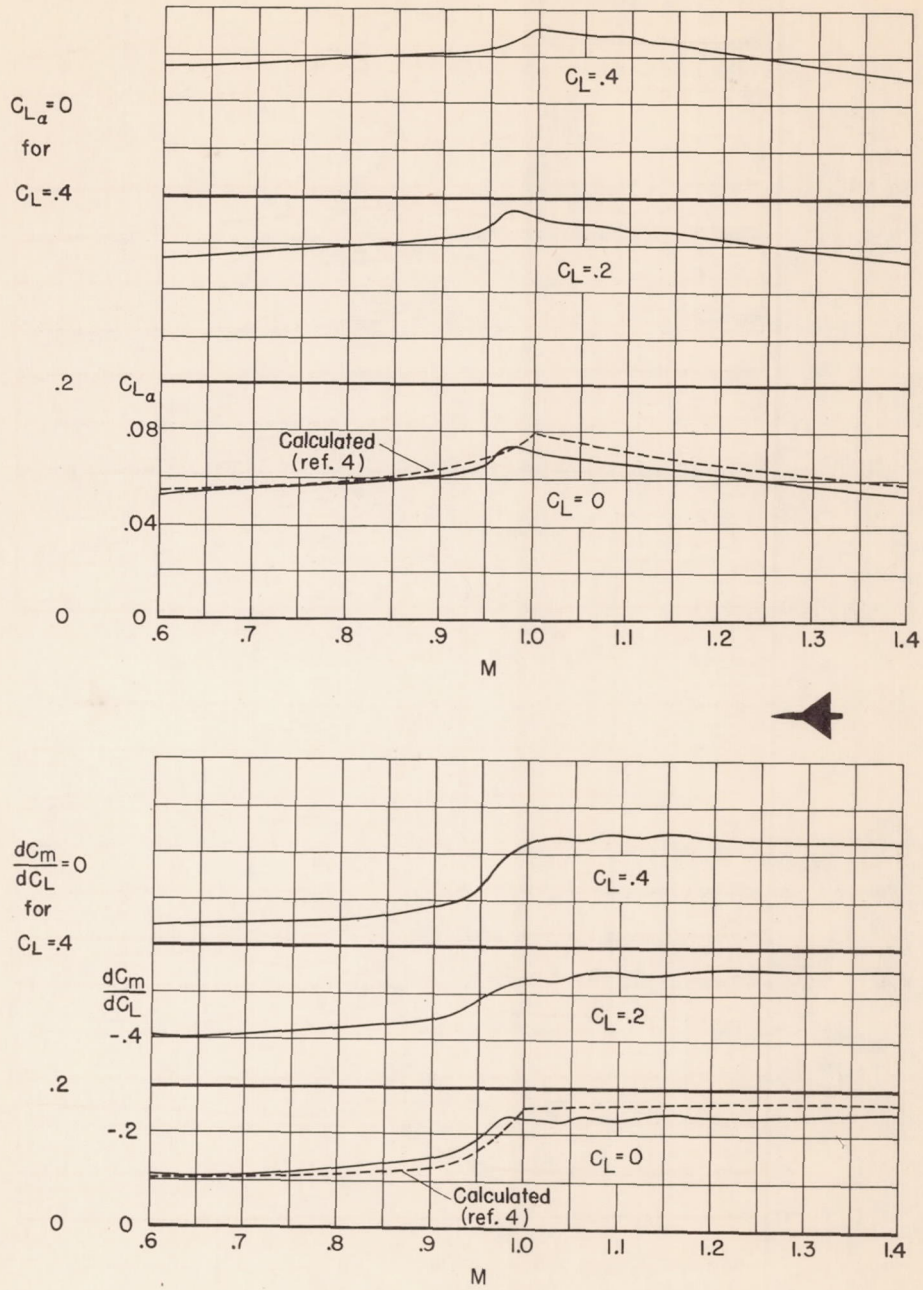

(e) $\Lambda = 53.1$, $\lambda = 0$.

Figure 7.- Concluded.

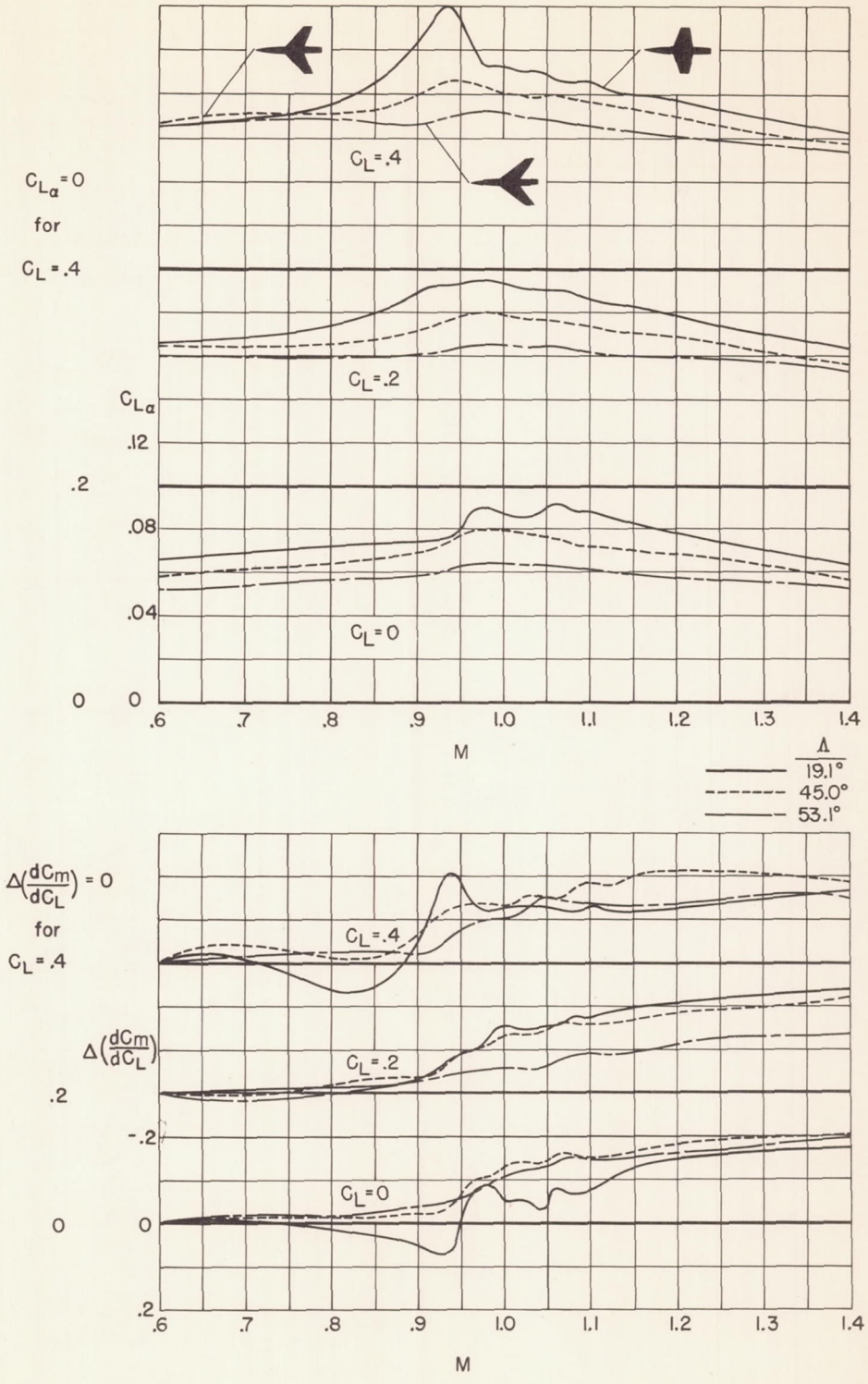

Figure 8.- Effect of sweep on the variation with Mach number of lift-curve slope and pitching-moment-curve slope; λ = 0.4.

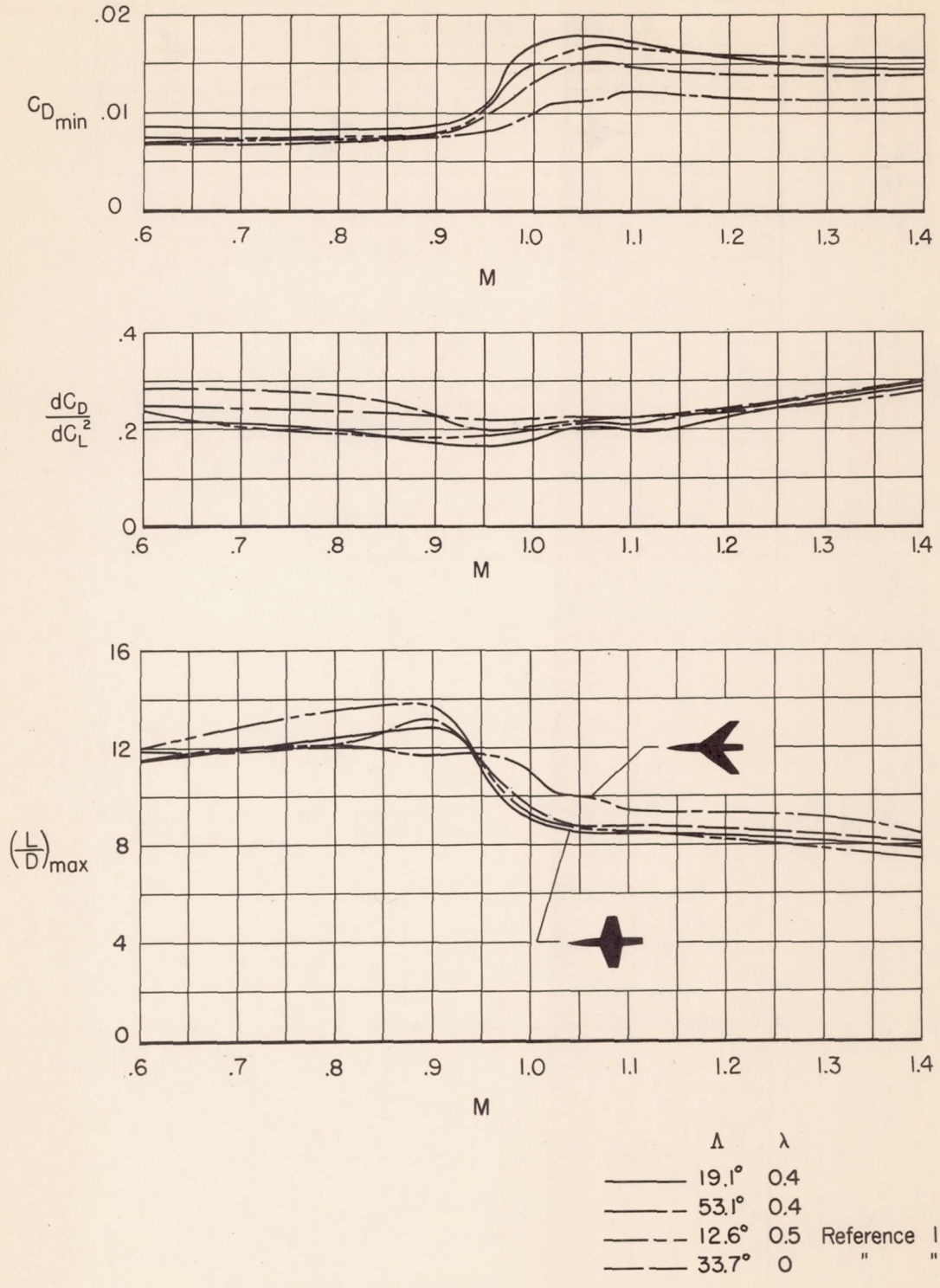

Figure 9.- Effect of sweep on the variation with Mach number of minimum drag coefficient, drag - rise factor, and maximum lift - drag ratio.

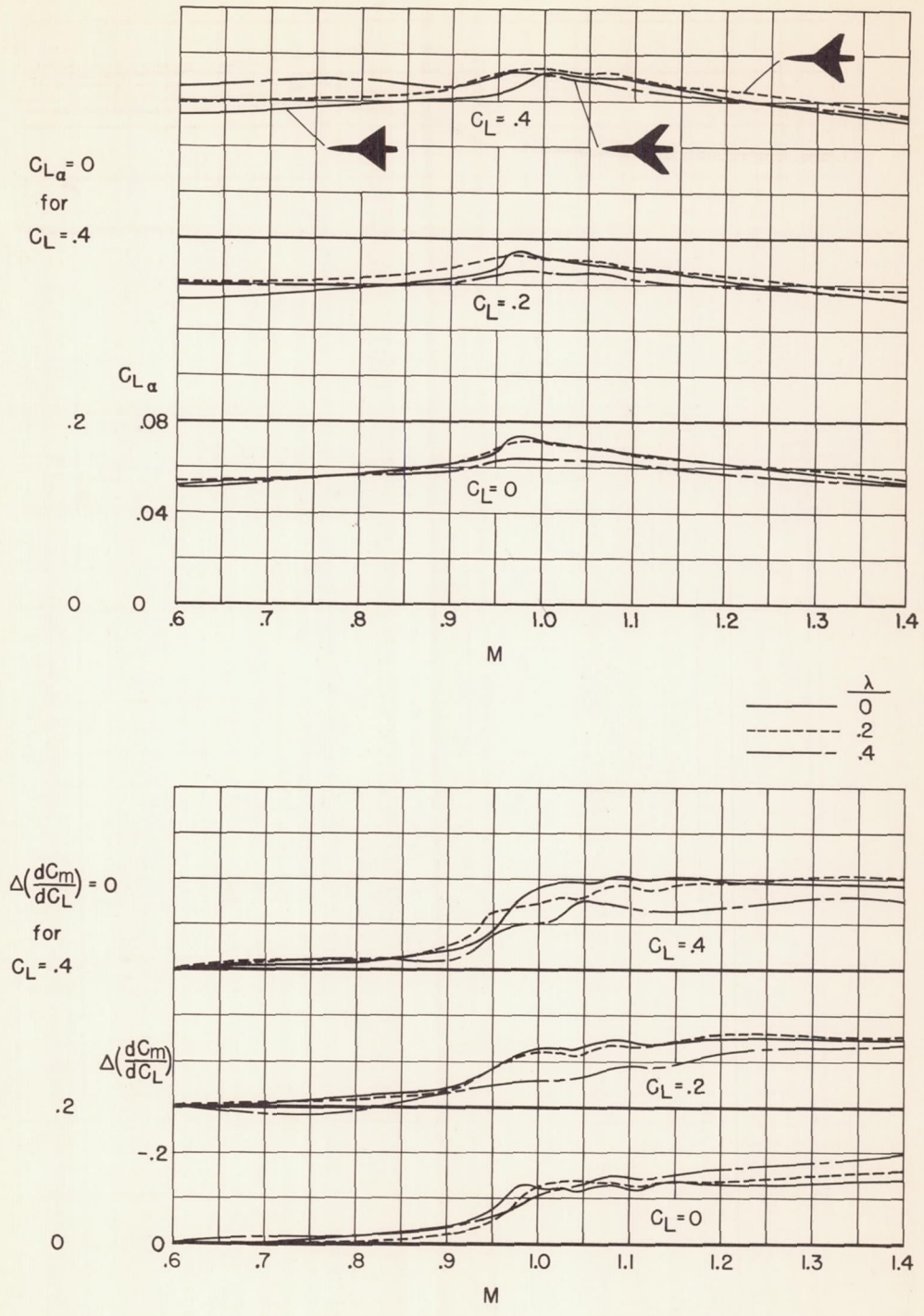

Figure 10.- Effect of taper ratio on the variation with Mach number of lift-curve slope and pitching-moment-curve slope; $\Lambda = 53.1°$.

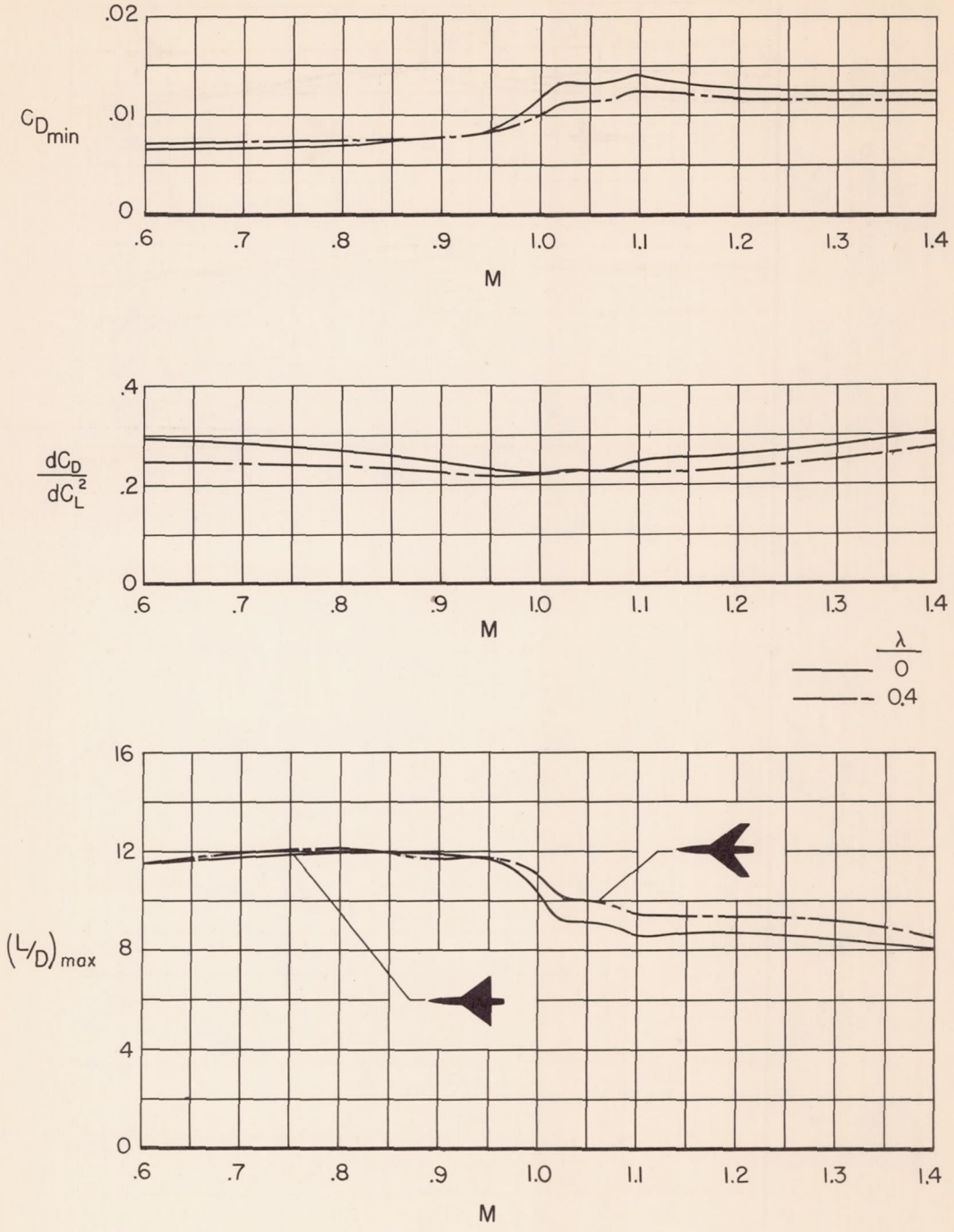

Figure 11.- Effect of taper ratio on the variation with Mach number of minimum drag coefficient, drag-rise factor, and maximum lift-drag ratio; $\Lambda = 53.1°$.

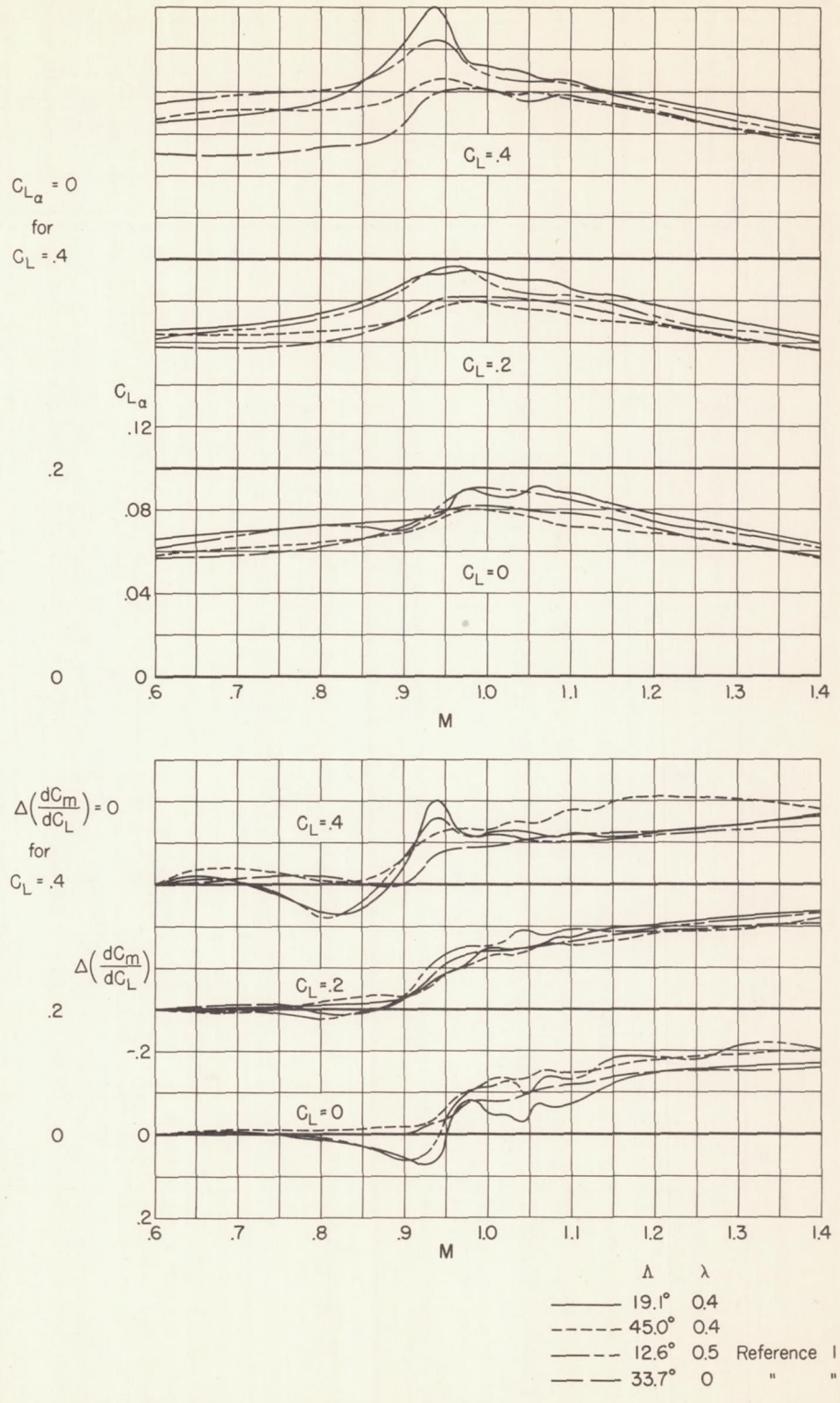

Figure 12.- Comparison of the effect of sweep as varied by two geometric methods on the variation with Mach number of lift-curve slope and pitching-moment-curve slope.

NACA-Langley - 3-23-55 - 350